

#### *Leptin as a profibrogenic cytokine via MAPK and PI3K/AKT*

Further, leptin increased TGF- $\beta$  mRNA in isolated sinusoidal endothelial cells and Kupffer cells. From this point of view, it is suggested that leptin promotes hepatic fibrogenesis through upregulation of TGF- $\beta$  in the liver. Moreover, leptin augmented PDGF-dependent proliferation of HSCs by enhancing downstream intracellular signaling pathways via mitogen-activated protein kinase (MAPK) and phosphatidylinositol 3 kinase (PI3K)/Akt.<sup>51</sup> Collectively, it is postulated that leptin acts as a profibrogenic cytokine in the sinusoidal microenvironment. These findings indicated that leptin is one of the key regulators for inflammation and progression of fibrosis in various chronic liver diseases including NASH. In a similar hypothesis, Anania et al. indicated that leptin is profibrogenic in activated HSCs partly via the Jak-Stat pathway as well.<sup>52</sup>

Recently, several studies also identified that leptin upregulates collagen expression in HSCs; i.e., increased  $\alpha 2$  (I) collagen gene expression in cultured rat hepatic stellate cells,<sup>53</sup> and enhanced  $\alpha 1$  (I) collagen gene expression in LX-2 human hepatic stellate cells via JAK-mediated H<sub>2</sub>O<sub>2</sub>-dependent MAPK pathways.<sup>54</sup> Meanwhile, several studies described that leptin stimulates and increases tissue inhibitor of metalloproteinase 1 (TIMP-1) gene expression.<sup>55-57</sup> Moreover, ObR activation in HSCs leads to increased expression of proinflammatory and proangiogenic cytokines, indicating a complex role for leptin in the regulation of liver wound-healing responses.<sup>58</sup> Collectively, it is most likely true that these data support the hypotheses: profibrogenesis is markedly increased when hepatic stellate cells are activated, where leptin plays a pivotal role in hepatic fibrosis.

#### *Mitochondria abnormalities and NAFLD/NASH*

Mitochondrial abnormalities were described in liver biopsy specimens of patients with NASH<sup>59,60</sup>; however, it is also unclear whether the observed mitochondrial abnormalities are congenital or acquired. Mitochondrial defects are supposed to be one of the primary causes of steatosis because of impaired  $\beta$ -oxidation of fatty acids in humans.<sup>61</sup> Moreover, recent study has shown that anti-TNF antibody improves mitochondrial dysfunction in ob/ob mice.<sup>62</sup> Taken together, these findings indicated that inflammation derived from oxidative stress is one of the most important backgrounds in patients with NAFLD/NASH as well as metabolic syndrome.

#### *Chronic hepatitis C, hepatic steatosis, and metabolic syndrome*

Chronic hepatitis C virus (HCV) infection is a significant worldwide problem because approximately 170 million people are suffering from HCV infection. It is thought that about 80% of acute HCV infection becomes chronic, that 20% will develop liver cirrhosis, and that 1%–6% will develop hepatocellular carcinoma each year.<sup>63</sup> A new treatment strategy including the combination of pegylated interferon and ribavirin were developed; nevertheless, the overall efficacy of the treatment is not enough to overcome HCV infection at the moment, as only about 54%–63% respond.<sup>64-66</sup>

Hepatic steatosis is a common histological feature of chronic hepatitis C (CHC), which is observed in 40%–70% of the patients.<sup>67</sup> Hepatic steatosis occurs more frequently in patients with chronic hepatitis C than in the general population in the world.<sup>68</sup> First, focusing epidemiologically on host-related factors, overweight patients with chronic hepatitis C have increased circulating insulin levels.<sup>69</sup> At the same time, obesity and diabetes mellitus and/or insulin resistance are associated with hepatic steatosis in patients with chronic hepatitis C.<sup>70-72</sup> These clinical features are often observed in patients with metabolic syndrome. Therefore, it was supposed that multiple risk factors for metabolic disorders are closely correlated with the prevalence of hepatic steatosis in CHC patients. Second, focusing on virus-related factors, it was commonly shown that the HCV genotype 3 is significantly associated with hepatic steatosis.<sup>73</sup> Additionally, evaluation of paired (pre- and postantiviral therapy) liver biopsies demonstrated a marked decline in steatosis in HCV genotype 3 patients who achieved sustained viral response (SVR).<sup>74</sup> Although it is hypothesized that genotype 3 virus is more cytopathic and therefore steatogenic, the mechanisms underlying the genotype specific steatosis are still not fully elucidated. Moreover, transgenic mice expressing hepatitis C virus core protein develop hepatic steatosis and insulin resistance without gain in body weight at a young age.<sup>75,76</sup> Taken together, these findings suggested that multiple factors are closely associated with the occurrence of hepatic steatosis in patients with chronic hepatitis C, not only host-related metabolic disorders but also HCV itself.

Importantly, emerging lines of clinical data revealed that several metabolic disturbances, such as obesity, insulin resistance, and hepatic steatosis, are significant risk factors for decreased SVR to the interferon and ribavirin combination antiviral therapy in CHC patients<sup>71,72,77-81</sup> (Table 1). Underlying mechanisms of lesser efficacy of antiviral treatment are not well investigated; however, it is postulated that oxidant stress and

**Table 1.** Relationships between hepatic steatosis and response rate of antiviral therapy in patients with chronic hepatitis C

Reference	Patient numbers (study design)	Treatment	Genotype (%)			SVR rate (%)		
			Fatty liver (%)			Fatty liver (%)		
			1	2	3	Overall	Fatty liver (+)	Fatty liver (-)
Bynard et al. <sup>70</sup> Hepatology 2003	1428 (retrospective)	48W IFN $\alpha$ -2b or 48W pegIFN $\alpha$ -2b plus Riba	68	15	15	54	35	57
Sanyal et al. <sup>59</sup> Am J Gastroenterol 2003	137 (retrospective)	IFN plus Riba or PegIFN alone or plus Riba	90	4	3	25	14	35
Romero-Gomez et al. <sup>60</sup> Gastroenterology 2005	159 (prospective)	Peg IFN plus Riba	71	23	6	52	18	53.7
Harrison et al. <sup>65</sup> Clin Gastroenterol Hepatol 2005	315 (retrospective)	IFN or pegIFN plus Riba	76	24		40	28 (>33% steatosis)	44 (<33% steatosis)
Thomopoulos et al. <sup>63</sup> J Gastroenterol Hepatol 2005	116 (retrospective)	IFN or pegIFN plus Riba	41	8	34	52	39	66
D'Souza et al. <sup>64</sup> Am J Gastroenterol 2005	59 (prospective)	Peg IFN 2 $\alpha$ plus Riba	63	genotype 1 and 2		55	55	56
Camma et al. <sup>71</sup> Hepatology 2006	291 (prospective)	Peg IFN plus Riba	100			36	25 (>1% steatosis)	50 (<1% steatosis)
Yaginuma et al. <sup>68</sup> Hepatol Res 2006	80 (retrospective)	24W IFN $\alpha$ -2b plus Riba	84	16		50	30 (>33% steatosis)	58 (<33% steatosis)
Jian et al. <sup>66</sup> Liver Int 2006	98 (prospective)	24W or 48W pegIFN $\alpha$ -2a plus Riba	39	45	13	58	29	62
Soresi et al. <sup>67</sup> Liver Int 2006	112 (prospective)	48W pegIFN $\alpha$ -2a plus Riba	72	14	13	41	33	55

IFN, interferon; pegIFN, pegylated interferon; Riba, ribavirin; SVR, sustained viral response; 48W, 48 weeks

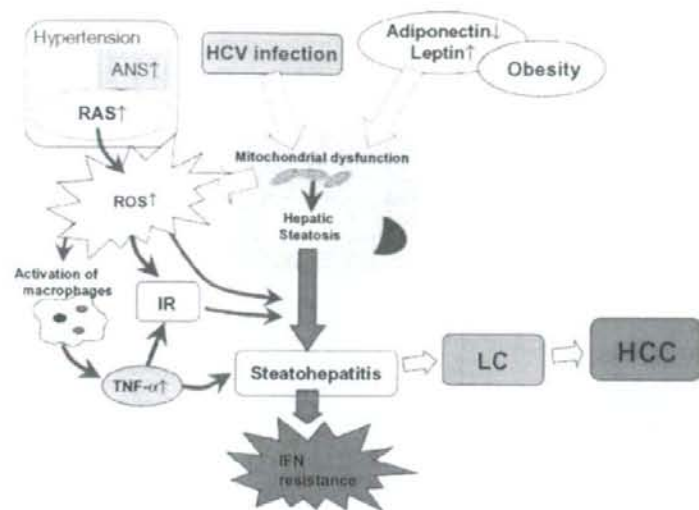


**Fig. 1.** Working hypothesis of the underlying mechanisms of the interaction between liver diseases including HCV infection and metabolic syndrome. (i) Underlying mechanisms of lesser efficacy of antiviral treatment are not well investigated; however, it is postulated that oxidant stress and proinflammatory cytokines are closely associated with interferon resistance. (ii) Etanercept, which is a chimerical protein that binds to and inactivates TNF- $\alpha$  in the liver and mononuclear cells, has been reported to improve the efficacy of antiviral treatment in patients with chronic hepatitis C. (iii) Furthermore, hepatic steatosis is a risk factor for HCC in patients with chronic HCV infection. *HCV*, hepatitis C virus; *ROS*, reactive oxygen species; *TNF- $\alpha$* , tumor necrosis factor- $\alpha$ ; *IFN*, interferon; *IR*, insulin resistance; *RAS*, renin-angiotensin system; *ANS*, autonomic nervous system; *HCC*, hepatocellular carcinoma

proinflammatory cytokines are closely associated with interferon resistance.<sup>88,89</sup> Indeed, Etanercept, which is a chimerical protein that binds to and inactivates TNF- $\alpha$  in the liver and mononuclear cells, has been reported to improve the efficacy of antiviral treatment in patients with chronic hepatitis C<sup>90</sup> (Fig. 1).

Collectively, it is most likely true that intensive adjustment of metabolic imbalance before the induction of antiviral therapy is favorable for the complete eradication of HCV infection.

#### Metabolic syndrome and progression of fibrosis, occurring as hepatocellular carcinoma (HCC) in chronic hepatitis

Progression of hepatic fibrosis is an important aspect in patients with chronic liver disease, such as NASH and chronic hepatitis C, because liver cirrhosis is one of the critical risk factors for liver-related death, including liver failure and hepatocellular carcinoma.

Recently, it has become apparent that hepatic fibrosis is associated with obesity, insulin resistance, and hepatic steatosis.<sup>91,92</sup> It is reported that NASH can progress to cirrhosis in up to 20% of the patients.<sup>93</sup> Therefore, it is suggested that metabolic abnormalities are closely associated with progression of fibrosis as well.

As a malignant disease, HCC is one of the most important diseases in patients with chronic liver disease. Recently, some epidemiological studies have reported that obesity and diabetes mellitus are a risk factor for hepatocellular carcinoma (HCC), respectively.<sup>94-96</sup> Furthermore, hepatic steatosis is a risk factor for HCC

in patients with chronic HCV infection as well<sup>97</sup> (Fig. 1).

In the meantime, experimental data suggested that *PTEN* deficiency leads to steatohepatitis and hepatocellular carcinoma.<sup>98</sup> *PTEN* is a ubiquitously expressed tumor suppressor gene<sup>99</sup> that is mutated in many human sporadic cancers as well as in tumorigenic hereditary disorders. It is postulated that controlled blocking of molecules acting downstream of PI3K might provide significant therapeutic benefit to patients predisposed to NASH and hepatocellular carcinoma.

#### Hepatic steatosis, atherosclerosis, and hypertension

Metabolic syndrome, which is characterized by insulin resistance, is associated with atherosclerosis and hypertension and is recognized as an inflammatory disease.<sup>100,101</sup> It is a serious disease because the mortality rate of cardiovascular disease is increasing, especially in Asia.<sup>102</sup>

As with liver disease, it was reported that hypo-adiponectinemia is observed in patients with coronary artery disease and is associated with the incidence of cardiovascular death.<sup>103,104</sup> Experimental data demonstrated that adenovirus-mediated increase of plasma adiponectin significantly suppressed the progression of atherosclerotic lesions in apolipoprotein E-deficient mice.<sup>105</sup>

Recently, the PROactive study (PROspective pioglitazone Clinical Trial In macroVascular Events) has shown that pioglitazone, agonists of peroxisome proliferators-activated receptor  $\gamma$  (PPAR- $\gamma$ ), which is a thiazolidinedione that ameliorates insulin resistance

and improves glucose and lipid metabolism in type 2 diabetes, reduces the composite of all-cause mortality, nonfatal myocardial infarction, and stroke in patients with type 2 diabetes who have a high risk of macrovascular events.<sup>106</sup>

Hepatic steatosis is also increasingly recognized as one of the important risk factors for atherosclerosis and cardiovascular disease<sup>107-109</sup> (Fig. 1). Interestingly, a recent prospective study has shown that histological features in patients with NASH: including hepatic steatosis, ballooning necrosis, and inflammation, are improved by administering pioglitazone as compared with placebo.<sup>110</sup> However, fatigue and mild lower-extremity edema developed in 1 of 55 subjects who received pioglitazone. Therefore, we have to find the appropriate dose of pioglitazone and be careful about the adverse effects.

Taken together, there seem to be close relationships among hepatic steatosis, atherosclerosis, and hypertension as metabolic disorders. From this point of view, we would be able to investigate the aspects of both liver and cardiovascular-related diseases.

## Conclusions

In this review, we described the current understanding of relationships between liver diseases and metabolic syndrome. As we noted, there are so many intricate factors of causing hepatic inflammation, steatosis/steatohepatitis, fibrosis, and carcinoma in patients with chronic liver diseases in conjunction with metabolic syndrome. We should pay a critical attention to "liver diseases," because there must be a clue to elucidate the pathophysiology of so-called metabolic syndrome.

Necessarily, to avoid developing fatal diseases in the end, we have to establish a radical treatment strategy not only by ordinary diet and exercise therapy but also developing a sure remedy against liver diseases and metabolic syndrome.

## References

- Executive Summary of The Third Report of The National Cholesterol Education Program (NCEP) Expert Panel on Detection, Evaluation, and Treatment of High Blood Cholesterol In Adults (Adult Treatment Panel III). *JAMA* 2001;285:2486-97.
- Eckel RH, Grundy SM, Zimmet PZ. The metabolic syndrome. *Lancet* 2005;365:1415-28.
- Watanabe S, Hojo M, Nagahara A. Metabolic syndrome and gastrointestinal diseases. *J Gastroenterol* 2007;42:267-74.
- Angulo P. Nonalcoholic fatty liver disease. *N Engl J Med* 2002;346:1221-31.
- Clark JM, Brancati FL, Diehl AM. Nonalcoholic fatty liver disease. *Gastroenterology* 2002;122:1649-57.
- Ludwig J, Viggiano TR, McGill DB, Oh BJ. Nonalcoholic steatohepatitis: Mayo Clinic experiences with a hitherto unnamed disease. *Mayo Clin Proc* 1980;55:434-8.
- Mokdad AH, Serdula MK, Dietz WH, Bowman BA, Marks JS, Koplan JP. The spread of the obesity epidemic in the United States, 1991-1998. *JAMA* 1999;282:1519-22.
- Mokdad AH, Bowman BA, Ford ES, Vinicor F, Marks JS, Koplan JP. The continuing epidemics of obesity and diabetes in the United States. *JAMA* 2001;286:1195-200.
- Marchesini G, Brizi M, Bianchi G, Tomassetti S, Bugianesi E, Lenzi M, et al. Nonalcoholic fatty liver disease: a feature of the metabolic syndrome. *Diabetes* 2001;50:1844-50.
- Pagano G, Pacini G, Musso G, Gambino R, Mecca F, DePetris N, et al. Nonalcoholic steatohepatitis, insulin resistance, and metabolic syndrome: further evidence for an etiologic association. *Hepatology* 2002;35:367-72.
- Marchesini G, Bugianesi E, Forlani G, Cerrelli F, Lenzi M, Manini R, et al. Nonalcoholic fatty liver, steatohepatitis, and the metabolic syndrome. *Hepatology* 2003;37:917-23.
- Day CP, James OF. Steatohepatitis: a tale of two "hits"? *Gastroenterology* 1998;114:842-5.
- Brunt EM, Janney CG, Di Bisceglie AM, Neuschwander-Tetri BA, Bacon BR. Nonalcoholic steatohepatitis: a proposal for grading and staging the histological lesions. *Am J Gastroenterol* 1999;94:2467-74.
- Matteoni CA, Younossi ZM, Gramlich T, Boparai N, Liu YC, McCullough AJ. Nonalcoholic fatty liver disease: a spectrum of clinical and pathological severity. *Gastroenterology* 1999;116:1413-9.
- Neuschwander-Tetri BA, Caldwell SH. Nonalcoholic steatohepatitis: summary of an AASLD Single Topic Conference. *Hepatology* 2003;37:1202-19.
- Kleiner DE, Brunt EM, Van Natta M, Behling C, Contos MJ, Cummings OW, et al. Design and validation of a histological scoring system for nonalcoholic fatty liver disease. *Hepatology* 2005;41:1313-21.
- Browning JD, Szczepaniak LS, Dobbins R, Nuremberg P, Horton JD, Cohen JC, et al. Prevalence of hepatic steatosis in an urban population in the United States: impact of ethnicity. *Hepatology* 2004;40:1387-95.
- Adams LA, Lymp JF, St Sauver J, Sanderson SO, Lindor KD, Feldstein A, et al. The natural history of nonalcoholic fatty liver disease: a population-based cohort study. *Gastroenterology* 2005;129:113-21.
- Powell EE, Cooksley WG, Hanson R, Searle J, Halliday JW, Powell LW. The natural history of nonalcoholic steatohepatitis: a follow-up study of forty-two patients for up to 21 years. *Hepatology* 1990;11:74-80.
- Bacon BR, Farahvash MJ, Janney CG, Neuschwander-Tetri BA. Nonalcoholic steatohepatitis: an expanded clinical entity. *Gastroenterology* 1994;107:1103-9.
- Teli MR, James OF, Burt AD, Bennett MK, Day CP. The natural history of nonalcoholic fatty liver: a follow-up study. *Hepatology* 1995;22:1714-9.
- Farrell GC, Larter CZ. Nonalcoholic fatty liver disease: from steatosis to cirrhosis. *Hepatology* 2006;43:S99-S112.
- Hamauchi M, Kojima T, Takeda N, Nakagawa T, Taniguchi H, Fujii K, et al. The metabolic syndrome as a predictor of nonalcoholic fatty liver disease. *Ann Intern Med* 2005;143:722-8.
- Axen KV, Dikeakos A, Sclafani A. High dietary fat promotes syndrome X in nonobese rats. *J Nutr* 2003;133:2244-9.
- Hill JO, Lin D, Yakubu F, Peters JC. Development of dietary obesity in rats: influence of amount and composition of dietary fat. *Int J Obes Relat Metab Disord* 1992;16:321-33.
- Carmiel-Haggi M, Cederbaum AI, Nieto N. A high-fat diet leads to the progression of non-alcoholic fatty liver disease in obese rats. *FASEB J* 2005;19:136-8.
- Zhang Y, Proenca R, Maffei M, Barone M, Leopold L, Friedman JM. Positional cloning of the mouse obese gene and its human homologue. *Nature (Lond)* 1994;372:425-32.

28. Lee GH, Proenca R, Montez JM, Carroll KM, Darvishzadeh JG, Lee JI, et al. Abnormal splicing of the leptin receptor in diabetic mice. *Nature (Lond)* 1996;379:632-5.
29. Chen H, Charlat O, Tartaglia LA, Woolf EA, Weng X, Ellis SJ, et al. Evidence that the diabetes gene encodes the leptin receptor: identification of a mutation in the leptin receptor gene in db/db mice. *Cell* 1996;84:491-5.
30. Takaya K, Ogawa Y, Isse N, Okazaki T, Satoh N, Masuzaki H, et al. Molecular cloning of rat leptin receptor isoform complementary DNAs: identification of a missense mutation in Zucker fatty (fa/fa) rats. *Biochem Biophys Res Commun* 1996;225:75-83.
31. Chitturi S, Abeygunasekera S, Farrell GC, Holmes-Walker J, Hui JM, Fung C, et al. NASH and insulin resistance: Insulin hypersecretion and specific association with the insulin resistance syndrome. *Hepatology* 2002;35:373-9.
32. James O, Day C. Non-alcoholic steatohepatitis: another disease of affluence. *Lancet* 1999;353:1634-6.
33. Tsochatzidis E, Papatheodoridis GV, Archimandritis AJ. The evolving role of leptin and adiponectin in chronic liver diseases. *Am J Gastroenterol* 2006;101:2629-40.
34. Tilg H, Hotamisligil GS. Nonalcoholic fatty liver disease: Cytokine-adipokine interplay and regulation of insulin resistance. *Gastroenterology* 2006;131:934-45.
35. Hotamisligil GS, Shargill NS, Spiegelman BM. Adipose expression of tumor necrosis factor- $\alpha$ : direct role in obesity-linked insulin resistance. *Science* 1993;259:87-91.
36. Crespo J, Cayon A, Fernandez-Gil P, Hernandez-Guerra M, Mayorga M, Dominguez-Diez A, et al. Gene expression of tumor necrosis factor  $\alpha$  and TNF-receptors, p55 and p75, in nonalcoholic steatohepatitis patients. *Hepatology* 2001;34:1158-63.
37. Feldstein AE, Werneburg NW, Canbay A, Guicciardi ME, Bronk SF, Rydzewski R, et al. Free fatty acids promote hepatic lipotoxicity by stimulating TNF- $\alpha$  expression via a lysosomal pathway. *Hepatology* 2004;40:185-94.
38. Li Z, Yang S, Lin H, Huang J, Watkins PA, Moser AB, et al. Probiotics and antibodies to TNF inhibit inflammatory activity and improve nonalcoholic fatty liver disease. *Hepatology* 2003;37:343-50.
39. Arita Y, Kihara S, Ouchi N, Takahashi M, Maeda K, Miyagawa J, et al. Paradoxical decrease of an adipose-specific protein, adiponectin, in obesity. *Biochem Biophys Res Commun* 1999;257:79-83.
40. Kubota N, Terauchi Y, Yamauchi T, Kubota T, Moroi M, Matsui J, et al. Disruption of adiponectin causes insulin resistance and neointimal formation. *J Biol Chem* 2002;277:25863-6.
41. Kumada M, Kihara S, Sumitsuji S, Kawamoto T, Matsumoto S, Ouchi N, et al. Association of hypoadiponectinemia with coronary artery disease in men. *Arterioscler Thromb Vasc Biol* 2003;23:85-9.
42. Hui JM, Hodge A, Farrell GC, Kench JG, Kriketos A, George J. Beyond insulin resistance in NASH: TNF- $\alpha$  or adiponectin? *Hepatology* 2004;40:46-54.
43. Maeda N, Shimomura I, Kishida K, Nishizawa H, Matsuda M, Nagaretani H, et al. Diet-induced insulin resistance in mice lacking adiponectin/ACRP30. *Nat Med* 2002;8:731-7.
44. Xu A, Wang Y, Keshaw H, Xu LY, Lam KS, Cooper GJ. The fat-derived hormone adiponectin alleviates alcoholic and nonalcoholic fatty liver diseases in mice. *J Clin Invest* 2003;112:91-100.
45. Tartaglia LA, Dembski M, Weng X, Deng N, Culpepper J, Devos R, et al. Identification and expression cloning of a leptin receptor, OB-R. *Cell* 1995;83:1263-71.
46. Potter JJ, Wornack L, Mezey F, Anania FA. Transdifferentiation of rat hepatic stellate cells results in leptin expression. *Biochem Biophys Res Commun* 1998;244:178-82.
47. Ikejima K, Honda H, Yoshikawa M, Hirose M, Kitamura T, Takei Y, et al. Leptin augments inflammatory and profibrogenic responses in the murine liver induced by hepatotoxic chemicals. *Hepatology* 2001;34:288-97.
48. Honda H, Ikejima K, Hirose M, Yoshikawa M, Lang T, Enomoto N, et al. Leptin is required for fibrogenic responses induced by thioacetamide in the murine liver. *Hepatology* 2002;36:12-21.
49. Leclercq IA, Farrell GC, Schriener R, Robertson GR. Leptin is essential for the hepatic fibrogenic response to chronic liver injury. *J Hepatol* 2002;37:206-13.
50. Ikejima K, Takei Y, Honda H, Hirose M, Yoshikawa M, Zhang YJ, et al. Leptin receptor-mediated signaling regulates hepatic fibrogenesis and remodeling of extracellular matrix in the rat. *Gastroenterology* 2002;122:1399-410.
51. Ikejima K, Okumura K, Lang T, Honda H, Abe W, Yamashina S, et al. The role of leptin in progression of non-alcoholic fatty liver disease. *Hepatology Res* 2005;33:151-4.
52. Saxena NK, Ikeda K, Rockey DC, Friedman SL, Anania FA. Leptin in hepatic fibrosis: evidence for increased collagen production in stellate cells and lean littermates of ob/ob mice. *Hepatology* 2002;35:762-71.
53. Saxena NK, Saliba G, Floyd JJ, Anania FA. Leptin induces increased  $\alpha$ 2(I) collagen gene expression in cultured rat hepatic stellate cells. *J Cell Biochem* 2003;89:311-20.
54. Cao Q, Mak KM, Lieber CS. Leptin enhances  $\alpha$ 1(I) collagen gene expression in LX-2 human hepatic stellate cells through JAK-mediated H2O2-dependent MAPK pathways. *J Cell Biochem* 2006;97:188-97.
55. Cao Q, Mak KM, Ren C, Lieber CS. Leptin stimulates tissue inhibitor of metalloproteinase-1 in human hepatic stellate cells: respective roles of the JAK/STAT and JAK-mediated H2O2-dependent MAPK pathways. *J Biol Chem* 2004;279:4292-304.
56. Lin S, Saxena NK, Ding X, Stein LL, Anania FA. Leptin increases tissue inhibitor of metalloproteinase 1 (TIMP-1) gene expression by a specificity protein 1/signal transducer and activator of transcription 3 mechanism. *Mol Endocrinol* 2006;20:3376-88.
57. Cao Q, Mak KM, Lieber CS. Leptin represses matrix metalloproteinase-1 gene expression in LX2 human hepatic stellate cells. *J Hepatol* 2007;46:124-33.
58. Aleffi S, Petrai I, Bertolani C, Parola M, Colombatto S, Novo E, et al. Upregulation of proinflammatory and proangiogenic cytokines by leptin in human hepatic stellate cells. *Hepatology* 2005;42:1339-48.
59. Sanyal AJ, Campbell-Sargent C, Mirshahi F, Rizzo WB, Contos MJ, Sterling RK, et al. Nonalcoholic steatohepatitis: association of insulin resistance and mitochondrial abnormalities. *Gastroenterology* 2001;120:1183-92.
60. Caldwell SH, Swerdlow RH, Khan EM, Iezzoni JC, Hespender EE, Parks JK, et al. Mitochondrial abnormalities in non-alcoholic steatohepatitis. *J Hepatol* 1999;31:430-4.
61. Lowell BB, Shulman GI. Mitochondrial dysfunction and type 2 diabetes. *Science* 2005;307:384-7.
62. Garcia-Ruiz I, Rodriguez-Juan C, Diaz-Sanjuan T, del Hoyo P, Colina F, Munoz-Yague T, et al. Uric acid and anti-TNF antibody improve mitochondrial dysfunction in ob/ob mice. *Hepatology* 2006;44:581-91.
63. Seeff LB. Natural history of chronic hepatitis C. *Hepatology* 2002;36:S35-46.
64. Fried MW, Shiffman ML, Reddy KR, Smith C, Marinos G, Goncalves FL Jr, et al. Peginterferon alfa-2a plus ribavirin for chronic hepatitis C virus infection. *N Engl J Med* 2002;347:975-82.
65. Hadziyannis SJ, Sette H, Jr., Morgan TR, Balan V, Diago M, Marcellin P, et al. Peginterferon- $\alpha$ 2a and ribavirin combination therapy in chronic hepatitis C: a randomized study of treatment duration and ribavirin dose. *Ann Intern Med* 2004;140:346-55.
66. Manns MP, McHutchison JG, Gordon SC, Rustgi VK, Shiffman M, Reindollar R, et al. Peginterferon alfa-2b plus ribavirin compared with interferon alfa-2b plus ribavirin for initial treatment

- of chronic hepatitis C: a randomised trial. *Lancet* 2001;358: 958-65.
67. Ramesh S, Sanyal AJ. Hepatitis C and nonalcoholic fatty liver disease. *Semin Liver Dis* 2004;24:399-413.
68. Lonardo A, Adinolfi LE, Loria P, Carulli N, Ruggiero G, Day CP. Steatosis and hepatitis C virus: mechanisms and significance for hepatic and extrahepatic disease. *Gastroenterology* 2004;126: 586-97.
69. Hickman JJ, Powell EE, Prins JB, Clouston AD, Ash S, Purdie DM, et al. In overweight patients with chronic hepatitis C, circulating insulin is associated with hepatic fibrosis: implications for therapy. *J Hepatol* 2003;39:1042-8.
70. Monto A, Alonzo J, Watson JJ, Grunfeld C, Wright TL. Steatosis in chronic hepatitis C: relative contributions of obesity, diabetes mellitus, and alcohol. *Hepatology* 2002;36: 729-36.
71. Camma C, Bruno S, Di Marco V, Di Bona D, Rumi M, Vinci M, et al. Insulin resistance is associated with steatosis in nondiabetic patients with genotype 1 chronic hepatitis C. *Hepatology* 2006;43:64-71.
72. Conjeevaram HS, Kleiner DE, Everhart JE, Hoofnagle JH, Zacks S, Afdhal NH, et al. Race, insulin resistance and hepatic steatosis in chronic hepatitis C. *Hepatology* 2007;45:80-7.
73. Rubbia-Brandt L, Quadri R, Abid K, Giostra E, Male PJ, Mentha G, et al. Hepatocyte steatosis is a cytopathic effect of hepatitis C virus genotype 3. *J Hepatol* 2000;33:106-15.
74. Patton HM, Patel K, Behling C, Bylund D, Blatt LM, Vallee M, et al. The impact of steatosis on disease progression and early and sustained treatment response in chronic hepatitis C patients. *J Hepatol* 2004;40:484-90.
75. Moriya K, Yotsuyanagi H, Shintani Y, Fujie H, Ishibashi K, Matsuura Y, et al. Hepatitis C virus core protein induces hepatic steatosis in transgenic mice. *J Gen Virol* 1997;78(pt 7):1527-31.
76. Shintani Y, Fujie H, Miyoshi H, Tsutsumi T, Tsukamoto K, Kimura S, et al. Hepatitis C virus infection and diabetes: direct involvement of the virus in the development of insulin resistance. *Gastroenterology* 2004;126:840-8.
77. Bressler BL, Guindi M, Tomlinson G, Heathcote J. High body mass index is an independent risk factor for nonresponse to antiviral treatment in chronic hepatitis C. *Hepatology* 2003;38: 639-44.
78. Charlton MR, Pockros PJ, Harrison SA. Impact of obesity on treatment of chronic hepatitis C. *Hepatology* 2006;43:1177-86.
79. Poynard T, Ratziu V, McHutchison J, Manns M, Goodman Z, Zeuzem S, et al. Effect of treatment with peginterferon or interferon alpha-2b and ribavirin on steatosis in patients infected with hepatitis C. *Hepatology* 2003;38:75-85.
80. Sanyal AJ, Contos MJ, Sterling RK, Luketic VA, Shiffman ML, Stravitz RT, et al. Nonalcoholic fatty liver disease in patients with hepatitis C is associated with features of the metabolic syndrome. *Am J Gastroenterol* 2003;98:2064-71.
81. Romero-Gomez M, Del Mar Viloria M, Andrade RJ, Salmeron J, Diago M, Fernandez-Rodriguez CM, et al. Insulin resistance impairs sustained response rate to peginterferon plus ribavirin in chronic hepatitis C patients. *Gastroenterology* 2005;128: 636-41.
82. Harrison SA, Brunt EM, Qazi RA, Oliver DA, Neuschwander-Tetri BA, Di Bisceglie AM, et al. Effect of significant histologic steatosis or steatohepatitis on response to antiviral therapy in patients with chronic hepatitis C. *Clin Gastroenterol Hepatol* 2005;3:604-9.
83. Thomopoulos KC, Theocharis GJ, Tsimantzas AC, Singris D, Dimitropoulou D, Gogos CA, et al. Liver steatosis is an independent risk factor for treatment failure in patients with chronic hepatitis C. *Eur J Gastroenterol Hepatol* 2005;17:149-53.
84. D'Souza R, Sabin CA, Foster GR. Insulin resistance plays a significant role in liver fibrosis in chronic hepatitis C and in the response to antiviral therapy. *Am J Gastroenterol* 2005;100: 1509-15.
85. Yaginuma R, Ikejima K, Okumura K, Kon K, Suzuki S, Takei Y, et al. Hepatic steatosis is a predictor of poor response to interferon alpha-2b and ribavirin combination therapy in Japanese patients with chronic hepatitis C. *Hepatol Res* 2006;35: 19-25.
86. Jian Wu Y, Shu Chen L, Gui Qiang W. Effects of fatty liver and related factors on the efficacy of combination antiviral therapy in patients with chronic hepatitis C. *Liver Int* 2006; 26:166-72.
87. Soresi M, Tripi S, Franco V, Giannitrapani L, Alessandri A, Rappa F, et al. Impact of liver steatosis on the antiviral response in the hepatitis C virus-associated chronic hepatitis. *Liver Int* 2006;26:1119-25.
88. Larrea E, Garcia N, Qian C, Civeira MP, Prieto J. Tumor necrosis factor alpha gene expression and the response to interferon in chronic hepatitis C. *Hepatology* 1996;23:210-7.
89. Di Bona D, Cipitelli M, Fionda C, Camma C, Licata A, Santoni A, et al. Oxidative stress inhibits IFN-alpha-induced antiviral gene expression by blocking the JAK-STAT pathway. *J Hepatol* 2006;45:271-9.
90. Zein NN. Etanercept as an adjuvant to interferon and ribavirin in treatment-naive patients with chronic hepatitis C virus infection: a phase 2 randomized, double-blind, placebo-controlled study. *J Hepatol* 2005;42:315-22.
91. Angulo P, Keach JC, Batts KP, Lindor KD. Independent predictors of liver fibrosis in patients with nonalcoholic steatohepatitis. *Hepatology* 1999;30:1356-62.
92. Dixon JB, Bhathal PS, O'Brien PE. Nonalcoholic fatty liver disease: predictors of nonalcoholic steatohepatitis and liver fibrosis in the severely obese. *Gastroenterology* 2001;121:91-100.
93. McCullough AJ. The clinical features, diagnosis and natural history of nonalcoholic fatty liver disease. *Clin Liver Dis* 2004; 8:521-33, viii.
94. Caldwell SH, Crespo DM, Kang HS, Al-Osaimi AM. Obesity and hepatocellular carcinoma. *Gastroenterology* 2004;127:S97-103.
95. El-Serag HB, Tran T, Everhart JE. Diabetes increases the risk of chronic liver disease and hepatocellular carcinoma. *Gastroenterology* 2004;126:460-8.
96. Davila JA, Morgan RO, Shaib Y, McGlynn KA, El-Serag HB. Diabetes increases the risk of hepatocellular carcinoma in the United States: a population based case control study. *Gut* 2005;54:533-9.
97. Ohata K, Hamasaki K, Toriyama K, Matsumoto K, Saeki A, Yanagi K, et al. Hepatic steatosis is a risk factor for hepatocellular carcinoma in patients with chronic hepatitis C virus infection. *Cancer (Phila)* 2003;97:3036-43.
98. Horie Y, Suzuki A, Kataoka E, Sasaki T, Hamada K, Sasaki J, et al. Hepatocyte-specific Pten deficiency results in steatohepatitis and hepatocellular carcinomas. *J Clin Invest* 2004;113: 1774-83.
99. Li J, Yen C, Liaw D, Podyspanina K, Bose S, Wang S, et al. PTEN, a putative protein tyrosine phosphatase gene mutated in human brain, breast, and prostate cancer. *Science* 1997;275: 1943-7.
100. Ferrannini E, Buzzigoli G, Bonadonna R, Giorico MA, Oleggini M, Graziadei L, et al. Insulin resistance in essential hypertension. *N Engl J Med* 1987;317:350-7.
101. Ross R. Atherosclerosis: an inflammatory disease. *N Engl J Med* 1999;340:115-26.
102. Nestel P, Lyu R, Low LP, Sheu WH, Nitiyanant W, Saito I, et al. Metabolic syndrome: recent prevalence in East and Southeast Asian populations. *Asia Pac J Clin Nutr* 2007;16:362-7.
103. Ouchi N, Kihara S, Ariga Y, Maeda K, Kuriyama H, Okamoto Y, et al. Novel modulator for endothelial adhesion molecules: adipocyte-derived plasma protein adiponectin. *Circulation* 1999; 100:2473-6.
104. Zoccali C, Mallamaci F, Tripepi G, Benedetto FA, Cutrupi S, Parlongo S, et al. Adiponectin, metabolic risk factors, and cir-

- diovascular events among patients with end-stage renal disease. *J Am Soc Nephrol* 2002;13:134-41.
105. Okamoto Y, Kihara S, Ouchi N, Nishida M, Arita Y, Kumada M, et al. Adiponectin reduces atherosclerosis in apolipoprotein E-deficient mice. *Circulation* 2002;106:2767-70.
106. Dormandy JA, Charbonnel B, Eckland DJ, Erdmann E, Massi-Benedetti M, Moules IK, et al. Secondary prevention of macrovascular events in patients with type 2 diabetes in the PROactive Study (PROspective pioglitAZone Clinical Trial In macroVascular Events): a randomised controlled trial. *Lancet* 2005;366:1279-89.
107. Dichl AM. Fatty liver, hypertension, and the metabolic syndrome. *Gut* 2004;53:923-4.
108. Sanyal AJ, Banas C, Sargeant C, Luketic VA, Sterling RK, Stravitz RT, et al. Similarities and differences in outcomes of cirrhosis due to nonalcoholic steatohepatitis and hepatitis C. *Hepatology* 2006;43:682-9.
109. Donati G, Stagni B, Piscaglia F, Venturoli N, Morselli-Labate AM, Rasciti L, et al. Increased prevalence of fatty liver in arterial hypertensive patients with normal liver enzymes: role of insulin resistance. *Gut* 2004;53:1020-3.
110. Belfort R, Harrison SA, Brown K, D'Arland C, Finch J, Hardies J, et al. A placebo-controlled trial of pioglitazone in subjects with nonalcoholic steatohepatitis. *N Engl J Med* 2006;355:2297-307.

# Translocation of Iron from Lysosomes into Mitochondria Is a Key Event During Oxidative Stress-Induced Hepatocellular Injury

Akira Uchiyama,<sup>1,2</sup> Jae-Sung Kim,<sup>3</sup> Kazuyoshi Kon,<sup>2</sup> Hartmut Jaeschke,<sup>4</sup> Kenichi Ikejima,<sup>2</sup> Sumio Watanabe,<sup>2</sup> and John J. Lemasters<sup>1,5</sup>

Iron overload exacerbates various liver diseases. In hepatocytes, a portion of non-heme iron is sequestered in lysosomes and endosomes. The precise mechanisms by which lysosomal iron participates in hepatocellular injury remain uncertain. Here, our aim was to determine the role of intracellular movement of chelatable iron in oxidative stress-induced killing to cultured hepatocytes from C3Heb mice and Sprague-Dawley rats. Mitochondrial polarization and chelatable iron were visualized by confocal microscopy of tetramethylrhodamine methylester (TMRM) and quenching of calcein, respectively. Cell viability and hydroperoxide formation (a measure of lipid peroxidation) were measured fluorometrically using propidium iodide and chloromethyl dihydrodichlorofluorescein, respectively. After collapse of lysosomal/endosomal acidic pH gradients with bafilomycin (50 nM), an inhibitor of the vacuolar proton-pumping adenosine triphosphatase, cytosolic calcein fluorescence became quenched. Deferoxamine mesylate and starch-deferoxamine (1 mM) prevented bafilomycin-induced calcein quenching, indicating that bafilomycin induced release of chelatable iron from lysosomes/endosomes. Bafilomycin also quenched calcein fluorescence in mitochondria, which was blocked by 20  $\mu$ M Ru360, an inhibitor of the mitochondrial calcium uniporter, consistent with mitochondrial iron uptake by the uniporter. Bafilomycin alone was not sufficient to induce mitochondrial depolarization and cell killing, but in the presence of low-dose *tert*-butylhydroperoxide (25  $\mu$ M), bafilomycin enhanced hydroperoxide generation, leading to mitochondrial depolarization and subsequent cell death. **Conclusion:** Taken together, the results are consistent with the conclusion that bafilomycin induces release of chelatable iron from lysosomes/endosomes, which is taken up by mitochondria. Oxidative stress and chelatable iron thus act as two "hits" synergistically promoting toxic radical formation, mitochondrial dysfunction, and cell death. This pathway of intracellular iron translocation is a potential therapeutic target against oxidative stress-mediated hepatotoxicity. (HEPATOLOGY 2008;48:1644-1654.)

Chelatable iron and other transition metals such as copper catalyze formation of highly reactive hydroxyl radical ( $\text{OH}^\bullet$ ) from  $\text{H}_2\text{O}_2$  and superoxide ( $\text{O}_2^{\bullet-}$ ), which damages DNA, proteins, and mem-

branes.<sup>1</sup> Cytoprotection by deferoxamine in various models of oxidative stress and hypoxia/ischemia suggests a role for iron in the pathogenesis of injury.<sup>2-6</sup> In hepatocytes, generation of reactive oxygen species (ROS), including

*Abbreviations:* cmDCF, chloromethyl dichlorofluorescein; cmH<sub>2</sub>DCF-DA, chloromethyl dihydrodichlorofluorescein diacetate; HEPES, 4-(2-hydroxyethyl)-1-piperazine ethanesulfonic acid; MPT, mitochondrial permeability transition;  $\text{O}_2^{\bullet-}$ , superoxide;  $\text{OH}^\bullet$ , hydroxyl radical; PI, propidium iodide; ROS, reactive oxygen species; *t*-BuOOH, *tert*-butylhydroperoxide; TMRM, tetramethylrhodamine methylester.

From the <sup>1</sup>Departments of Pharmaceutical & Biomedical Sciences, Medical University of South Carolina, Charleston, SC; the <sup>2</sup>Department of Gastroenterology, Juntendo University School of Medicine, Tokyo, Japan; the <sup>3</sup>Department of Surgery, University of Florida, Gainesville, FL; the <sup>4</sup>Department of Pharmacology, Toxicology & Therapeutics, University of Kansas Medical Center, Kansas City, KS; and the <sup>5</sup>Department of Biochemistry & Molecular Biology, Medical University of South Carolina, Charleston, SC.

Received November 18, 2007; accepted June 18, 2008.

Supported in part by grants DK070125, DK073336, DK37054, and C06 RR015435 from the National Institutes of Health.

Address reprint requests to: Dr. John J. Lemasters, Departments of Pharmaceutical & Biomedical Sciences and Biochemistry & Molecular Biology, Medical University of South Carolina, 280 Calhoun Street, MSC 140, Charleston, SC 29425. E-mail: jlemasters@musc.edu; fax: 843-792-1617.

Copyright © 2008 by the American Association for the Study of Liver Diseases.

Published online in Wiley InterScience (www.interscience.wiley.com).

DOI: 10.1002/hep.22498

Potential conflict of interest: Nothing to report.



$H_2O_2$ ,  $O_2^{\bullet -}$ , and  $OH^{\bullet}$ , contributes to lethal cell injury from oxidative stress, various hepatotoxicants, and ischemia/reperfusion.<sup>7-9</sup> In particular, ROS formation initiates onset of the mitochondrial permeability transition (MPT) caused by opening of nonspecific permeability transition pores in the mitochondrial inner membrane.<sup>5,10</sup> Open permeability transition pores conduct all solutes up to 1500 Da to cause mitochondrial depolarization, uncoupling of oxidative phosphorylation, and large-amplitude mitochondrial swelling. These events lead either to necrosis from adenosine triphosphate depletion or apoptosis from release of pro-apoptotic proteins such as cytochrome *c*.

Although an essential nutrient, iron in excess is a human toxicant causing acute hepatocellular necrosis after accidental overdose and chronic hepatic injury in hereditary hemochromatosis.<sup>11</sup> Excess iron also may aggravate diabetes, cancer, cardiovascular disease, and alcoholic and nonalcoholic steatohepatitis.<sup>12-16</sup> In cells and tissues, two pools of iron exist. The first pool is "non-chelatable" iron that is sequestered in ferritin or in structural components of proteins (such as heme, iron-sulfur complexes) and that cannot be removed by conventional iron chelators such as deferoxamine. The second pool is "chelatable" iron that represents free iron and iron bound less strongly to a wide variety of anionic intracellular molecules. Estimated to be 5  $\mu$ M in hepatocytes,<sup>17</sup> chelatable iron is accessible to deferoxamine and other iron chelators. Increases of intracellular chelatable iron contribute to death of sinusoidal endothelial cells and hepatocytes after cold ischemia/reperfusion.<sup>18,19</sup> Moreover, direct addition to hepatocytes of a membrane-permeable  $Fe^{3+}$  complex causes the MPT and consequent necrotic and apoptotic cell killing,<sup>20</sup> whereas the iron chelator *N,N,N',N'*-tetrakis(2-pyridylmethyl)ethylenediamine attenuates caspase activation and apoptosis in posts ischemic livers.<sup>21</sup>

The precise mechanisms by which iron is mobilized to contribute to hepatocellular injury after oxidative and other stresses remain poorly understood. Here using laser scanning confocal microscopy, we show that lysosomes are a source of rapidly mobilized chelatable iron and that chelatable iron released by lysosomes is rapidly taken up into mitochondria by the calcium uniporter. Inside mitochondria, this iron is available to catalyze toxic ROS cascades.

## Materials and Methods

**Hepatocyte Isolation and Culture.** All experiments were conducted using protocols approved by the Institutional Animal Care and Use Committee. Hepatocytes were isolated from 25 to 30 g overnight-fasted male

C3Heb/FeJ mice (Jackson Laboratory, Bar Harbor, ME) and 200 to 250 g overnight-fasted male Sprague-Dawley rats (Charles River, Wilmington, MA) by collagenase perfusion, as described previously.<sup>22</sup> Hepatocytes were resuspended in Waymouth's medium MB-752/1 (GIBCO, Grand Island, NY) containing 2 mM L-glutamine, 10% fetal bovine serum, 100 nM insulin (Squibb-Novo, Princeton, NJ), 100 nM dexamethasone (LyphoMed, Rosemont, IL), 100 units/mL penicillin, and 100  $\mu$ g/mL streptomycin. Cell viability was greater than 92%, as determined by trypan blue exclusion. Hepatocytes were plated in 24-well microtiter plates ( $1.5 \times 10^5$  cells per well) and 35-mm Petri dishes ( $6.0 \times 10^5$  cells) with 14-mm glass coverslips for imaging (MatTek, Ashland, MA). Plates and coverslips were coated with 0.1% Type-1 rat-tail collagen (Sigma, St. Louis, MO). Hepatocytes were allowed to attach for 4 hours in humidified 5%  $CO_2$ , 95% air at 37°C. Subsequently, hepatocytes were washed once and incubated in Waymouth's medium 752/1 containing 20 mM N-2-hydroxyethyl-piperazine-N'-2'-ethanesulfonic acid (HEPES, Sigma) buffer supplemented with 10% fetal bovine serum, 100 nM insulin, 100 nM dexamethasone, 100 units/mL penicillin, and 100  $\mu$ g/mL streptomycin at pH 7.4 (Waymouth/HEPES).

**Fluorometric Assay of Cell Viability and ROS.** After attachment to 24-well plates, mouse hepatocytes were washed once and replaced with Waymouth/HEPES containing 30  $\mu$ M propidium iodide (PI, Molecular Probes/Invitrogen, Eugene, OR) or 10  $\mu$ M chloromethylchlorodichlorofluorescein diacetate (cmH<sub>2</sub>DCF-DA, Molecular Probes/Invitrogen). Cell killing (PI) and ROS production (cmH<sub>2</sub>DCF-DA) were assessed using a multiwell fluorescence plate reader (BMG Lab Technologies, Germany), as previously described.<sup>23,24</sup> Increased PI fluorescence correlates closely with trypan blue uptake, whereas as conversion of de-esterified nonfluorescent cmH<sub>2</sub>DCF-DA to green fluorescing chloromethylchlorofluorescein (cmDCF) signifies production of organic hydroperoxides that are formed after lipid peroxidation.<sup>25</sup> Fluorescence does not arise from a direct reaction with  $H_2O_2$ . Rather, cmDCF fluorescence is a general indicator of ROS production and not an indicator for a specific species of oxygen radical.

In some experiments, hepatocytes were preincubated 1 hour with 1 mM deferoxamine (Sigma), 1 mM deferoxamine conjugated to hydroxyethylstarch (starch-deferoxamine, >10 kDa, Biomedical Frontiers, Minneapolis, MN) or 20  $\mu$ M Ru360 (Calbiochem, San Diego, CA) at 37°C. After pretreatment, hepatocytes were then incubated for 1 hour in the presence and absence of 50 nM bafilomycin A1 (Calbiochem) before addition of *tert*-butylhydroperoxide (*t*-BuOOH, 25  $\mu$ M, Sigma).

**Loading of Fluorophores.** Hepatocytes plated on

glass coverslips in Waymouth/HEPES were loaded for 20 minutes with calcein-AM (1  $\mu$ M, Molecular Probes/Invitrogen) or 10  $\mu$ M cmH<sub>2</sub>DCF-DA or tetramethylrhodamine methylester (TMRM, 100 nM, Molecular Probes/Invitrogen). The hepatocytes were then incubated in Waymouth/HEPES containing 300  $\mu$ M calcein-free acid, 50 nM TMRM, or 3  $\mu$ M PI, as indicated.

In some experiments, 70 kDa rhodamine-dextran (5 mg/100 g body weight, intraperitoneally, Sigma) was injected into rats 12 hours before hepatocyte isolation to label lysosomes.<sup>26</sup> After isolation, 6-hour cultured hepatocytes loaded with rhodamine-dextran were cold-loaded with 1  $\mu$ M calcein-AM for 1 hour at 4°C and washed. The cells were then incubated overnight in Waymouth/HEPES at 37°C. This procedure produced selective labeling of lysosomes with rhodamine-dextran and both mitochondria and lysosomes with calcein, as shown previously.<sup>27</sup>

**Laser Scanning Confocal Microscopy.** Hepatocytes loaded with the various combinations of fluorophores were placed in environmental chambers at 37°C on the stages of Zeiss LSM 410 and LSM 510 laser scanning confocal microscopes (Zeiss, Germany). Red fluorescence (TMRM, PI, Rho-Dex) was excited at 543 or 568 nm, and emission was imaged at > 590 nm. Green fluorescence (calcein, cmDCF) was excited at 488 nm, and emission was collected through a 515-nm to 560-nm band pass filter.

**Statistics.** Data are presented as means  $\pm$  standard error. Images shown are representative of three or more experiments. Statistical analysis was performed by Student *t* test or analysis of variance, using *P* < 0.05 as the criterion of significance.

## Results

### *Bafilomycin-Induced Increase of Chelatable Iron in the Cytosol.*

Cultured mouse hepatocytes were loaded with calcein, a fluorophore whose fluorescence is rapidly and stoichiometrically quenched by transition metal ions such as iron, copper, cobalt, and nickel.<sup>28</sup> Calcein-loaded hepatocytes were treated with bafilomycin (50 nM), an inhibitor of the vacuolar proton-pumping adenosine triphosphatase that collapses acidic lysosomal/endosomal pH gradients.<sup>29</sup> Bafilomycin caused quenching of calcein loaded into the cytosol that was evident within 60 minutes and even more marked after 2 hours (Fig. 1B). Loss of calcein fluorescence was not caused by passive leak into the extracellular medium, because calcein fluorescence decreased to substantially below the fluorescence of exogenous calcein-free acid (300  $\mu$ M) placed in the extracellular medium. Quenching of calcein fluorescence was a

specific effect of bafilomycin, because intracellular calcein fluorescence declined only slightly in hepatocytes not exposed to bafilomycin (Fig. 1A).

To determine whether quenching of calcein in the cytosol was a consequence of an increase of chelatable iron, hepatocytes were treated with deferoxamine or starch-deferoxamine before exposure to bafilomycin. Deferoxamine and starch-deferoxamine are specific iron chelators, but starch-deferoxamine is membrane-impermeable and can enter cells only via endocytosis. Deferoxamine and starch-deferoxamine (1 mM) both largely blocked calcein quenching after bafilomycin (Fig. 1C and D), which supported the conclusion that calcein quenching was iron mediated.

After background subtraction, average calcein fluorescence was quantified for individual hepatocytes in the various groups. In untreated hepatocytes, calcein fluorescence decreased 17% after 2 hours (Fig. 2). By contrast, after bafilomycin, calcein fluorescence decreased 54% (*P* < 0.01 versus untreated). Deferoxamine and starch-deferoxamine blocked bafilomycin-induced calcein quenching almost completely, and calcein fluorescence decreased by only 16% and 13%, respectively, after bafilomycin plus deferoxamine and bafilomycin plus starch-deferoxamine (*P* < 0.01 versus bafilomycin alone) (Fig. 2).

After the treatment with bafilomycin, cytosolic calcein was quenched but TMRM fluorescence remained essentially unchanged both with and without treatment with deferoxamine and starch-deferoxamine (Fig. 1). Thus, mitochondria remained polarized during up to 2 hours of incubation with bafilomycin, which indicated lack of onset of the MPT.

### *Contribution of Chelatable Iron to Cytotoxicity*

**After Oxidative Stress.** Mitochondrial glutathione peroxidase reduces *t*-BuOOH to *t*-butanol, which promotes mitochondrial oxidative stress by depleting reduced nicotinamide adenine dinucleotide phosphate, and glutathione.<sup>30</sup> When hepatocytes were exposed to a relatively low dose of *t*-BuOOH (25  $\mu$ M), little cell killing occurred, as evaluated by PI fluorometry (Fig. 3A). Similarly, bafilomycin alone caused no cell killing over untreated cells. However, the combination of *t*-BuOOH plus bafilomycin caused substantial cytotoxicity over either *t*-BuOOH or bafilomycin alone (Fig. 3A). Treatment with deferoxamine and starch-deferoxamine prevented cytotoxicity by *t*-BuOOH plus bafilomycin and restored cell killing to nearly the same as untreated cells (Fig. 3B).

**The MPT After *t*-BuOOH Plus Bafilomycin.** To further characterize cellular responses after *t*-BuOOH with and without bafilomycin, confocal microscopy was performed of mouse hepatocytes that were loaded with

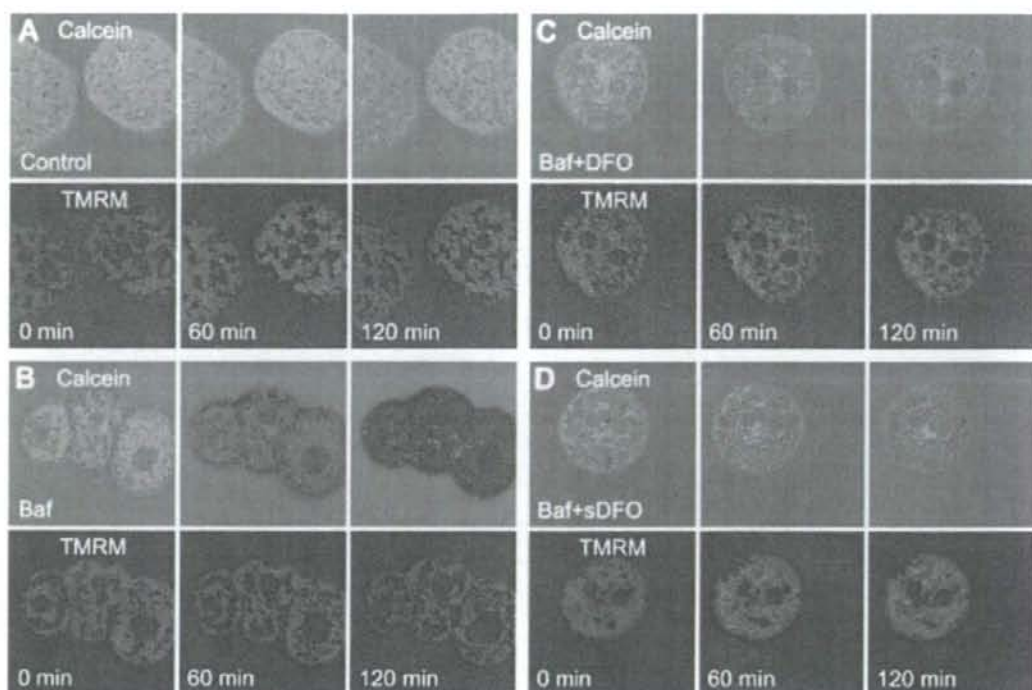


**Fig. 1.** Inhibition of bafilomycin-induced intracellular calcein quenching by deferoxamine and starch-deferoxamine in mouse hepatocytes. Mouse hepatocytes were co-loaded with TMRM (100 nM) and calcein-AM (1  $\mu$ M) and incubated with PI (3  $\mu$ M), calcein free acid (300  $\mu$ M), and TMRM (50 nM) in the extracellular medium with and without deferoxamine (1 mM) or starch-deferoxamine (1 mM deferoxamine equivalency), as described in Materials and Methods. Green fluorescence of calcein and red fluorescence of TMRM and PI were then imaged by laser scanning confocal microscopy before (0 minutes) and at 60 and 120 minutes after no further addition (A, Control), 50 nM bafilomycin (B, Baf), bafilomycin in the presence of deferoxamine (C, Baf+DFO) and bafilomycin in the presence of starch-deferoxamine (D, sBaf+DFO). Note the marked decrease of green calcein fluorescence in the cytosol in B after bafilomycin addition, which did not occur during the control incubation (A) and which was suppressed in the presence of deferoxamine (C) and starch-deferoxamine (D). TMRM fluorescence was maintained under all conditions, and PI did not label nuclei. Each experiment is typical of three or more replicates.

calcein and TMRM and then incubated in the presence of PI and calcein-free acid in the extracellular medium. After exposure to low-dose *t*-BuOOH (25  $\mu$ M) alone, virtually no loss of TMRM or quenching of calcein fluorescence occurred after 1 hour, although a small decrease of both calcein and TMRM fluorescence became evident after 2 hours (Fig. 4A). By contrast, after exposure to *t*-BuOOH plus bafilomycin together, all TMRM fluorescence was lost within 1 hour (Fig. 4B). In one of the three cells in the field, loss of viability had already occurred, as shown by nuclear staining with PI. In the remaining cells, calcein fluorescence was decreased, especially in the middle cell, showing large surface blebs as a sign of cellular stress. After 90 minutes, all cells in the field had lost viability, as shown by PI labeling and the equilibration of intracellular and extracellular calcein fluorescence. Nonetheless, calcein fluorescence inside nonviable cells was somewhat less than outside because of space-filling structures (for example,

endoplasmic reticulum and nuclei) within the dead cells (Fig. 4B). Complete loss of TMRM fluorescence followed by cell death was consistent with onset of the MPT, as shown previously for hepatocytes exposed to higher concentrations of *t*-BuOOH.<sup>50</sup>

#### Protection Against Mitochondrial Depolarization by Iron Chelators

Calcein-loaded and TMRM-loaded hepatocytes were pretreated with deferoxamine (1 mM) before exposure to *t*-BuOOH plus bafilomycin. In the presence of deferoxamine, mitochondria did not release TMRM fluorescence after up to 2 hours of incubation (Fig. 4C). Similarly, quenching of calcein fluorescence was much decreased in comparison with hepatocytes not treated with deferoxamine (Fig. 4C; compare with Fig. 4B). Moreover, the hepatocytes did not lose viability, as shown by the lack of nuclear staining with PI. Similarly, starch-deferoxamine blocked mitochondrial depolarization and calcein quenching (Fig. 4D). In this last experi-

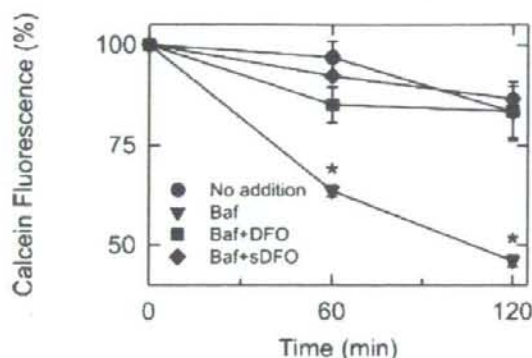


Fig. 2. Quantitation of calcein quenching after bafilomycin treatment. Mouse hepatocytes were loaded with calcein and treated as described in Fig. 1. Average calcein fluorescence of individual hepatocytes after background subtraction was determined at 60 and 120 minutes of incubation as the percentage of fluorescence before additions (0 minutes). Baf, bafilomycin; DFO, deferoxamine; sDFO, starch-deferoxamine; \* $P < 0.01$  compared with other groups ( $n = 2-5$  hepatocytes per group).

ment, TMRM had not yet fully equilibrated into mitochondria at the time of baseline imaging (Fig. 4D, 0 minutes), and TMRM fluorescence actually increased during incubation to reach stable steady-state mitochondrial loading. Thus, both iron chelators prevented the MPT and cell death induced by low-dose *t*-BuOOH plus bafilomycin.

**Formation of ROS After *t*-BuOOH Plus Bafilomycin.** To assess ROS formation after various treatments, we incubated mouse hepatocytes with  $\text{cmH}_2\text{DCF-DA}$  and measured development of hydroperoxide-indicating  $\text{cmDCF}$  fluorescence after exposure to bafilomycin, *t*-BuOOH, and bafilomycin plus *t*-BuOOH. Bafilomycin alone did not increase hydroperoxide formation at all in comparison with untreated hepatocytes (Fig. 5A). *t*-BuOOH alone caused an approximate doubling of the  $\text{cmDCF}$  signal in comparison with untreated cells. By contrast, the combination of bafilomycin plus *t*-BuOOH led to a fourfold increased signal (Fig. 5A). Iron chelation with either deferoxamine or starch-deferoxamine completely blocked hydroperoxide formation after bafilomycin plus *t*-BuOOH to levels observed in untreated cells (Fig. 5B).

**Lysosomal Integrity After Bafilomycin.** To this point, our findings strongly implicated the lysosomal/endosomal compartment as a source of mobilized chelatable iron, because bafilomycin increased cytosolic chelatable iron, as shown by calcein quenching. Moreover, starch deferoxamine, an iron chelator that gains entrance by endocytosis into the endosomal/lysosomal

compartment but not the cytosol, blocked the bafilomycin-induced increase of chelatable iron in the cytosol. Bafilomycin-induced release of chelatable iron suggested that iron was retained in lysosomes because of transport coupled to the pH gradient. Alternatively, bafilomycin may induce lysosomal swelling and rupture to cause iron release. To discriminate between these possibilities, lysosomes of rat hepatocytes were loaded with 70 kDa rhodamine-dextran. The mitochondria of the hepatocytes were also loaded with calcein, as described later. In untreated hepatocytes, rhodamine-dextran fluorescence persisted essentially unchanged for at least 2 hours (Fig. 6A, bottom panels). Although individual lysosomes moved in and out of the plane of section during the incubation, rhodamine-dextran fluorescence remained punctuate, and no release of red rhodamine-dextran fluorescence into the cytosol was observed. These findings confirmed the expectation that lysosomes remained intact during the

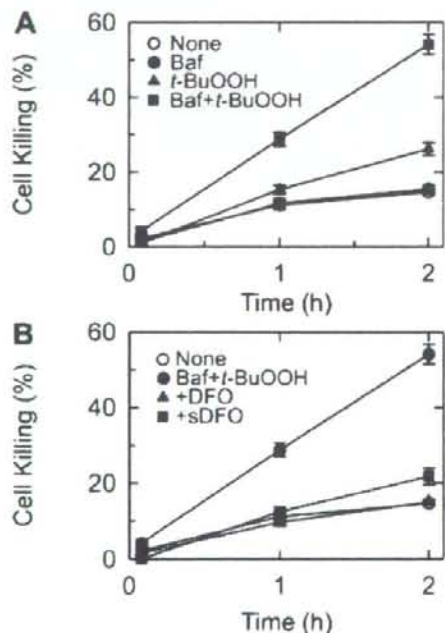


Fig. 3. Synergistic cell killing after bafilomycin plus *t*-BuOOH; protection by deferoxamine and starch-deferoxamine. Viability of mouse hepatocytes was assessed by PI fluorometry, as described in Materials and Methods. (A) Hepatocytes were exposed to *t*-BuOOH (25  $\mu\text{M}$ ) with and without 60 minutes of pretreatment with 50 nM bafilomycin (Baf). (B) Hepatocytes were treated with deferoxamine (1 mM) or starch-deferoxamine (1 mM deferoxamine equivalency) or no addition before bafilomycin plus *t*-BuOOH treatment. In both panels, "None" represents hepatocytes incubated without any additions. Values are means  $\pm$  standard error from three or more hepatocyte isolations.

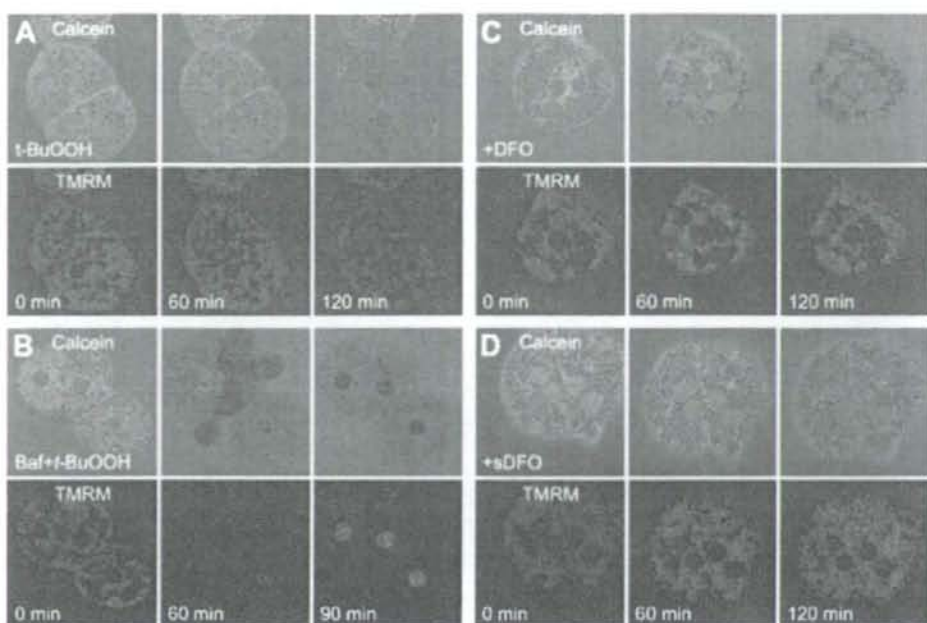


Fig. 4. Mitochondrial depolarization and cell death after bafilomycin plus *t*-BuOOH: protection by deferoxamine and starch-deferoxamine. Mouse hepatocytes were loaded, as described in Fig. 1, and exposed to 25  $\mu$ M *t*-BuOOH alone (A), *t*-BuOOH plus 50 nM bafilomycin (Baf) (B), *t*-BuOOH plus bafilomycin after pretreatment with deferoxamine (DFO, 1 mM) (C), and *t*-BuOOH plus bafilomycin after pretreatment with starch-deferoxamine (DFO, 1 mM deferoxamine equivalency) (D). After *t*-BuOOH alone (A), note that red mitochondrial TMRM fluorescence was retained and green calcein quenching did not occur. When *t*-BuOOH was combined with bafilomycin, calcein quenching, loss of TMRM, and cellular blebbing occurred within 60 minutes followed by nuclear PI labeling with 2 hours (B). Deferoxamine and starch-deferoxamine prevented calcein quenching, loss of TMRM fluorescence and nuclear labeling with PI (C and D). Each experiment is typical of three or more replicates.

normal incubation. Similarly after exposure to bafilomycin, rhodamine-dextran fluorescence remained punctate and did not move into the cytosol after as long as 2 hours (Fig. 6B, bottom panels). Thus, bafilomycin was not causing lysosomal fragility and rupture for at least 2 hours of observation. These results indicated that iron release was likely linked to bafilomycin-induced collapse of lysosomal/endosomal pH gradients rather than to disintegration of individual lysosomes.

**Increased Chelatable Iron in Mitochondria After Bafilomycin.** To assess whether chelatable iron released from lysosomes moves into mitochondria, we used a cold ester loading/warm incubation protocol to load calcein selectively into the mitochondria of rhodamine-dextran-loaded rat hepatocytes. When calcein-AM is loaded at colder temperatures into rat hepatocytes, mitochondrial esterases de-esterify a portion of the calcein-AM to trap calcein-free acid in the mitochondrial matrix as well as the cytosol.<sup>27,30</sup> Similarly, lysosomal esterases lead to lysosomal loading of calcein. Subsequent warm incubation overnight then causes loss of cytosolic calcein through an anion transporter in the plasma membrane, but mito-

chondrial and lysosomal calcein is retained. However, attempts to cold ester load calcein into the mitochondria of mouse hepatocytes were unsuccessful, possibly because of low activity of the mitochondrial esterase (data not shown). Accordingly, we continued these experiments using rat hepatocytes.

After calcein labeling of mitochondria and lysosomes by cold loading/warm incubation, compartmentation of calcein was quite stable during a normal incubation, and no redistribution of calcein from either organelle into the cytosol was observed even after 2 hours (Fig. 6A, top panels). By contrast, when hepatocytes were exposed to bafilomycin, mitochondrial calcein fluorescence progressively and substantially decreased over 2 hours (Fig. 6B, top panels). Calcein fluorescence in rhodamine-dextran-labeled lysosomes after bafilomycin did not decrease but instead appeared to increase (Fig. 6B, arrows). Thus, as inferred from calcein quenching and unquenching, bafilomycin caused lysosomal chelatable iron to decrease and mitochondrial chelatable iron to increase.

In hepatocytes co-loaded with rhodamine-dextran in lysosomes and calcein in both mitochondria and lyso-

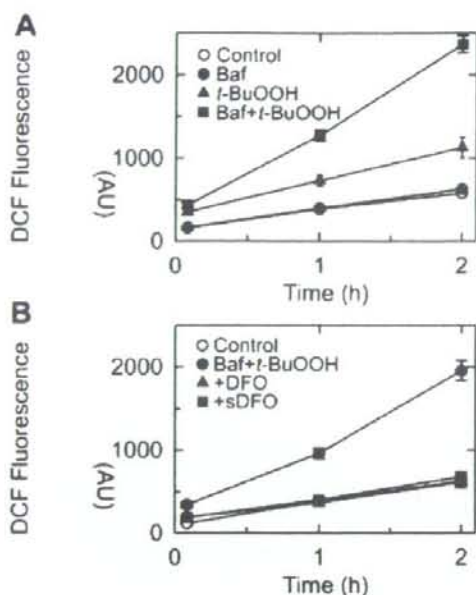


Fig. 5. ROS formation after bafilomycin plus t-BuOOH: protection by deferoxamine and starch-deferoxamine. Mouse hepatocytes were incubated with  $\text{cmH}_2\text{DCF-DA}$  ( $10 \mu\text{M}$ ), and fluorescence was measured using a fluorescence plate reader. (A) Hepatocytes were exposed to t-BuOOH ( $25 \mu\text{M}$ ) with and without 60 minutes pretreatment with  $50 \text{ nM}$  bafilomycin (Baf) in comparison with bafilomycin alone. (B) Hepatocytes were treated with deferoxamine (DFO,  $1 \text{ mM}$ ), starch-deferoxamine (sDFO,  $1 \text{ mM}$  deferoxamine equivalency), or no addition before bafilomycin plus t-BuOOH. In both panels, "Control" represents hepatocytes incubated without any additions. Values are means  $\pm$  standard error from three or more hepatocyte isolations.

somes, deferoxamine and starch-deferoxamine each suppressed bafilomycin-induced quenching of mitochondrial calcein fluorescence (Fig. 6C, D). Deferoxamine mesylate suppressed quenching of mitochondrial calcein fluorescence somewhat more strongly than starch-deferoxamine. Deferoxamine and starch-deferoxamine also promoted unquenching of lysosomal calcein fluorescence after bafilomycin over the course of 2 hours of incubation (Fig. 6C and D, arrows). Taken together, these findings indicated that quenching of calcein fluorescence in mitochondria after bafilomycin was attributable specifically to an increase of mitochondrial chelatable iron in association with a decrease in lysosomal chelatable iron.

**Iron Uptake Into Mitochondria by the Calcium Uniporter.** Ru360 is a highly specific inhibitor of the mitochondrial electrogenic calcium uniporter.<sup>31</sup> When hepatocytes were co-loaded with rhodamine-dextran in lysosomes and calcein in both mitochondria and lysosomes, exposure to bafilomycin in the presence of Ru360

( $20 \mu\text{M}$ ) decreased mitochondrial calcein quenching (Fig. 7). However, in contrast to deferoxamine and starch-deferoxamine, Ru360 did not induce an increase of calcein fluorescence in lysosomes (Fig. 7, arrows).

## Discussion

**Release of Lysosomal Iron Into the Cytosol by Bafilomycin.** The major finding of the current work was that the lysosomal/endosomal compartment of cultured hepatocytes is a reservoir of chelatable iron, which is released on inhibition of the proton-pumping vacuolar adenosine triphosphatase with bafilomycin (Fig. 1). Chelatable iron released into the cytosol was in part taken up into mitochondria via the electrogenic calcium uniporter residing in the mitochondrial inner membrane (Figs. 6, 7). Bafilomycin-induced release of chelatable iron acted synergistically with the oxidant t-BuOOH to augment hydroperoxide formation, onset of the MPT, and cell death (Figs. 3-5). Suppression of these effects by deferoxamine and starch-deferoxamine confirmed the specific role of chelatable iron in augmenting cytotoxicity.

**Quenching of Calcein Fluorescence by Ferrous Iron.** Transition metals rapidly and stoichiometrically quench calcein fluorescence with the relative potency:  $\text{Cu} > \text{Ni} > \text{Co} > \text{Fe}^{2+} > \text{Mn} > \text{Zn} > \text{Pb} > \text{Fe}^{3+} > \text{Ca}, \text{Mg}, \text{Hg}$ .<sup>32</sup> Although copper and cobalt quench calcein fluorescence, quenching after bafilomycin treatment was prevented by deferoxamine and starch-deferoxamine. These chelators are highly specific for iron and do not chelate copper, cobalt, or nickel.<sup>33</sup> Aluminum is the only other biologically relevant metal that is chelated by deferoxamine, but aluminum does not quench calcein fluorescence. Thus, calcein quenching most likely represents an increase of chelatable iron, specifically ferrous iron ( $\text{Fe}^{2+}$ ). The magnitude of increase of chelatable iron was substantial, because the decrease of intracellular calcein fluorescence was roughly the magnitude of the fluorescence of calcein ( $300 \mu\text{M}$ ) placed to the extracellular medium. Assuming a one-to-one stoichiometry of chelatable iron to quenched calcein, bafilomycin led to an increase of chelatable iron in the range of  $300 \mu\text{M}$ .

**Two-Hit Hypothesis of Iron-Catalyzed Hydroxyl Radical Formation.** In the presence of  $\text{H}_2\text{O}_2$  (and  $\text{O}_2^{\bullet}$  dismutating to  $\text{H}_2\text{O}_2$ ),  $\text{Fe}^{2+}$  catalyzes  $\text{OH}^{\bullet}$  formation and lipid peroxidation.<sup>1</sup> After bafilomycin, increased chelatable iron by itself was not sufficient to enhance ROS production (increased  $\text{cmDCF}$  formation) (Fig. 5), the MPT (mitochondrial depolarization) (Fig. 4), or cell killing (PI uptake) (Fig. 3). Rather, two "hits" of oxidant stress and increased chelatable iron were needed to promote ROS formation, the MPT, and cell killing. Lack of

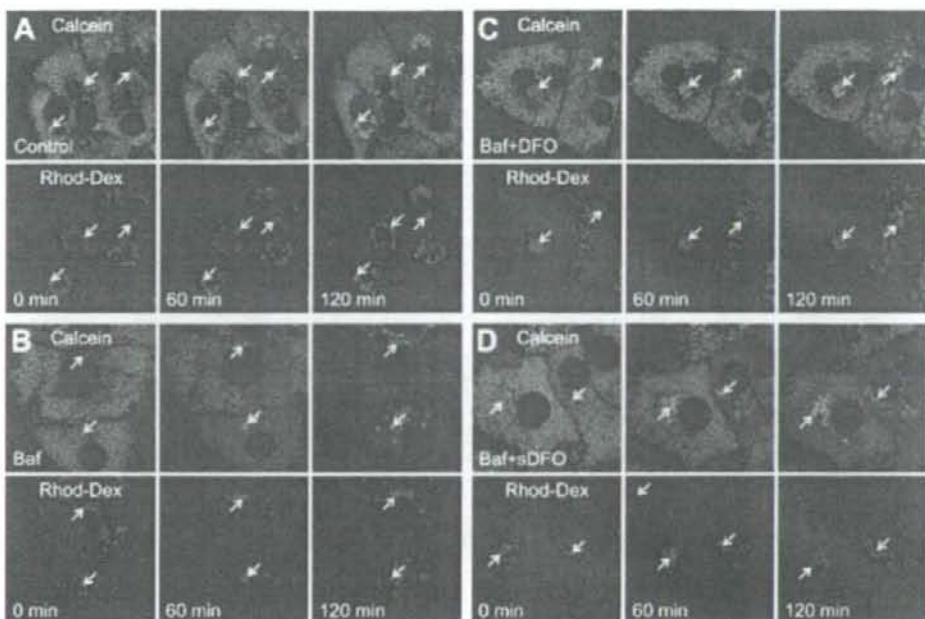


Fig. 6. Calcein quenching in mitochondria and unquenching in lysosomes after bafilomycin. Rat hepatocytes were loaded with 70 kDa rhodamine-dextran (Rhod-Dex) and co-loaded with calcein by cold ester loading/warm incubation, as described in Materials and Methods. The hepatocytes were then exposed to no addition (Control) (A), bafilomycin (Baf, 50 nM) (B), bafilomycin after pretreatment with deferoxamine (DFO, 1 mM) (C), and bafilomycin after pretreatment with starch-deferoxamine (sDFO, 1 mM deferoxamine equivalency) (D). Red fluorescence of rhodamine-dextran and green fluorescence of calcein were imaged by laser scanning confocal microscopy. Bafilomycin was added after collection of a baseline image (0 minutes) and then after 60 and 120 minutes. Note that mitochondrial calcein fluorescence and lysosomal rhodamine-dextran fluorescence did not change during the control incubation (A). By contrast, mitochondrial calcein was quenched markedly after bafilomycin, whereas lysosomal calcein fluorescence co-localizing with rhodamine-dextran appeared to increase (B). In the presence of deferoxamine (C) and starch-deferoxamine (D), mitochondrial calcein quenching was suppressed, whereas the increase of lysosomal calcein fluorescence appeared to be more marked. Rhodamine-dextran did not leak from lysosomes under any condition. Arrows identify representative lysosomal structures. Each experiment is typical of three or more replicates.

cytotoxicity after bafilomycin alone was not attributable to iron chelation by calcein, because cell killing and mitochondrial depolarization after bafilomycin did not occur in the absence of calcein loading (data not shown), which is consistent with the observation that most Fe-chelates are redox active, unlike deferoxamine.<sup>34</sup> Moreover, previous experiments with calcein did not show cytoprotection by the fluorophore.<sup>30</sup>

Mitochondrial iron overloading causing mitochondrial ROS formation, the MPT, and cell death may contribute to a variety of hepatic diseases, such as hepatotoxicity from iron overdose, hemochromatosis, and alcoholic and nonalcoholic steatohepatitis.<sup>12-14,16,55</sup> Direct addition of membrane-permeable iron complexes induces the MPT and killing of hepatocytes.<sup>20</sup> Moreover, in isolated mitochondria,  $\text{Fe}^{2+}$  induces the MPT at concentrations comparable to the approximately 300- $\mu\text{M}$  increase of chelatable iron observed here.<sup>36</sup> In conditions associated with lysosomal fragility and breakdown, such

as lipotoxicity and high cytokine exposure,<sup>57-60</sup> release of iron from lysosomes and uptake into mitochondria also may contribute to oxidative stress, MPT induction, and activation of death pathways. Similar mechanisms also play a role in Wilson's diseases, with copper replacing iron as the transition metal promoting oxidative stress.<sup>40</sup> These possibilities will need to be explored in future studies.

#### Cytoprotection by Deferoxamine and Starch-Deferoxamine via Chelation of Lysosomal Iron.

Deferoxamine is highly polar and poorly permeant through membranes, and high doses of deferoxamine (0.5-1 mM) are required to block hepatocyte killing after ischemia/reperfusion and oxidative stress, which may signify its poor penetration into the cytoplasm.<sup>41</sup> Alternatively, deferoxamine may enter through endocytosis into the acidic endosomal/lysosomal compartment, as has been suggested.<sup>42</sup> To assess the latter possibility, hepatocytes were exposed to bafilomycin in the presence of deferoxamine conjugated to hydroxyethyl starch (starch-deferoxamine,

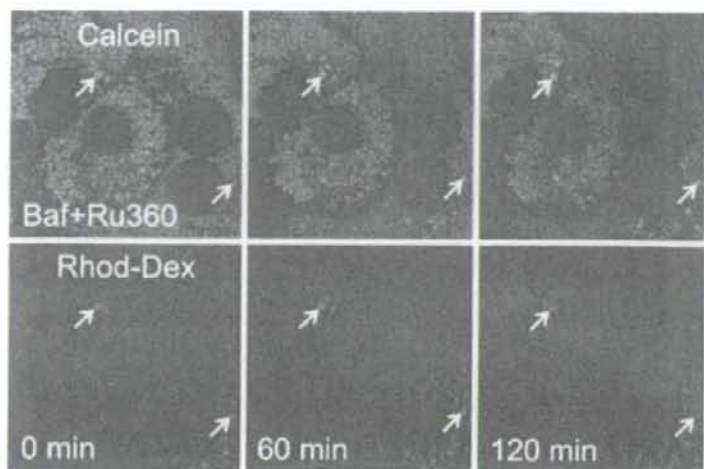


Fig. 7. Suppression of mitochondrial calcein quenching after bafilomycin by Ru360. Rat hepatocytes were loaded with rhodamine-dextran and calcein, as described in Fig. 6, and exposed to 50 nM bafilomycin (Baf) in the presence of 20  $\mu$ M Ru360. Note that in comparison to bafilomycin alone (Fig. 6B), mitochondrial calcein quenching was suppressed by Ru360. Arrows identify representative lysosomal structures. One experiment is typical of three or more replicates.

1 mM deferoxamine equivalency). The  $>10$  kDa starch-deferoxamine only enters cells by endocytosis. Strikingly, starch-deferoxamine prevented bafilomycin-induced calcein quenching as effectively as deferoxamine (Figs. 1, 2). These findings are consistent with the conclusion that lysosomes/endosomes release chelatable iron after bafilomycin and that deferoxamine and starch-deferoxamine prevent this release by chelating the intraluminal iron store of these organelles. Indeed, after calcein loading into lysosomes, bafilomycin treatment, especially in combination with deferoxamine or starch-deferoxamine, caused unquenching of calcein fluorescence, signifying a decrease of intraluminal chelatable iron within the lysosomes (Fig. 6). Other approaches to measuring changes of intraluminal lysosomal chelatable iron, such as homogenizing hepatocytes and isolating lysosomes by density gradient centrifugation, were considered but not pursued, because chelatable iron contained in lysosomes would most likely be released before the lysosomes could be purified.

***Fe<sup>2+</sup>/H<sup>+</sup> Exchange as a Mechanism of Lysosomal Iron Release.*** Changes of chelatable iron also may contribute to normal physiological processes. In Kupffer cells, chelatable iron increases transiently after lipopolysaccharide stimulation, and iron chelators block nuclear factor kappa B activation and cytokine formation.<sup>43-45</sup> Iron chelation also produces hypoxia inducible factor-1 $\alpha$  transactivation and expression of transferrin receptors.<sup>16a</sup> An important question is how intracellular iron is mobilized. Proteolysis in lysosomes and proteosomes recycles iron for biosynthetic reactions.<sup>46</sup> Similarly, heme oxygenase re-

leases iron as heme is degraded. Ferritin and hemosiderin store excess iron in a nonreactive highly chelated form. In plasma, transferrin binds almost all non-heme iron at two iron binding sites. Plasma transferrin is 5 to 10  $\mu$ M, and transferrin iron occupancy is approximately 30%, which translates to plasma iron of 3 to 6  $\mu$ M.<sup>49</sup> The endosomal/lysosomal compartment continuously receives iron by transferrin receptor-mediated endocytosis,<sup>50,51</sup> but how iron is released into the cytosol for cellular needs, such as synthesis of iron-containing proteins, is not known.<sup>52</sup> A membrane iron transporter, divalent metal transporter-1, mediates H<sup>+</sup>/Fe<sup>2+</sup> symport by enterocytes across the plasma membrane and early endosomes into the cytosol and may mediate iron release from lysosomes and late endosomes.<sup>52,53</sup> In our experiments, alkalinization of lysosomes/endosomes with bafilomycin caused release of chelatable iron into the cytosol without disrupting the integrity of individual lysosomes. This finding suggests that a Fe<sup>2+</sup>/H<sup>+</sup> exchange mechanism may be important in lysosomal iron retention at low lysosomal pH and release at high lysosomal pH.

During oxidative stress and hypoxia/ischemia, lysosomes rupture in hepatocytes and other cells.<sup>26,48,54,55</sup> In cell lines, lysosomal rupture is a source of iron release and consequent pro-oxidant cell damage.<sup>56-58</sup> Lysosomal degradation also occurs in models of apoptosis to hepatocytes.<sup>59</sup> Overall, chelatable iron may act both as a dynamic regulator of cellular function and as a mediator of cell injury. Like the better characterized calcium ion, chelatable iron may represent both a signal regulating normal



cellular responses and an intracellular mediator of toxicity when iron homeostasis is dysregulated.

**Mitochondrial Iron Uptake After Lysosomal Iron Release.** Using a technique of cold-loading followed by warm incubation, we were able to load mitochondria selectively with calcein (Fig. 6). After bafilomycin treatment, mitochondrial calcein fluorescence decreased, signifying an increase of chelatable iron within the mitochondria. Both deferoxamine and starch deferoxamine suppressed mitochondrial calcein quenching after bafilomycin (Fig. 6). Thus, chelatable iron released into the cytosol by bafilomycin from lysosomes and endosomes was being taken up into mitochondria.

Previous studies show that isolated mitochondria accumulate  $\text{Fe}^{2+}$  electrogenically via the mitochondrial  $\text{Ca}^{2+}$  uniporter.<sup>60</sup>  $\text{Fe}^{3+}$  is not transported. We confirmed this observation in intact hepatocytes by showing that Ru360, a highly specific inhibitor of the calcium uniporter,<sup>31</sup> inhibited bafilomycin-induced quenching of mitochondrial calcein fluorescence (Fig. 7). Thus, mitochondria took up at least a portion of chelatable iron released by lysosomes after bafilomycin via the calcium uniporter. In previous studies of ischemia/reperfusion injury and oxidative stress with t-BuOOH, ROS formation assessed with DCF occurred primarily within mitochondria.<sup>5,24</sup> Such ROS formation promoted onset of the MPT and subsequent cell death, because mitochondrial depolarization, inner membrane permeabilization, and loss of cell viability were blocked by deferoxamine and antioxidants.<sup>5,24</sup> Thus, the two hits of ROS generation and increased chelatable iron may be occurring within mitochondria to promote the MPT and cell death.

In conclusion, iron potentiates injury in a variety of diseases of the liver and other organs. Storage of chelatable iron in the lysosomal compartment and the mobilization of lysosomal iron by various stressors may be important events exacerbating hepatocellular injury. In particular, injury from oxidant stress may involve the two "hits" to mitochondria of increased  $\text{O}^{\bullet-}/\text{H}_2\text{O}_2$  and increased chelatable iron to promote formation of highly reactive and toxic  $\text{OH}^{\bullet}$ . Understanding of these mechanisms may lead to new strategies to minimize iron-dependent hepatocellular injury in various liver diseases.

## References

- Kehler JP. The Haber-Weiss reaction and mechanism of toxicity. *Toxicology* 2000;149:13-50.
- Starke PE, Farber JL. Ferric iron and superoxide ions are required for the killing of cultured hepatocytes by hydrogen peroxide: evidence for the participation of hydroxyl radicals formed by an iron-catalyzed Haber-Weiss reaction. *J Biol Chem* 1985;260:10099-10104.
- Kyle ME, Micaleli S, Nakae D, Farber JL. Superoxide dismutase and catalase protect cultured hepatocytes from the cytotoxicity of acetaminophen. *Biochem Biophys Res Commun* 1987;149:889-896.
- Dawson TL, Gores GJ, Nieminen AL, Herman B, Lemasters JJ. Mitochondria as a source of reactive oxygen species during reductive stress in rat hepatocytes. *Am J Physiol* 1993;264:C961-C967.
- Nieminen AL, Byrne AM, Herman B, Lemasters JJ. Mitochondrial permeability transition in hepatocytes induced by t-BuOOH: NAD(P)H and reactive oxygen species. *Am J Physiol* 1997;272:C1286-C1294.
- Lemasters JJ. Rusty notions of cell injury. *J Hepatol* 2004;40:696-698.
- Jeschke H, Gores GJ, Cederbaum AI, Hinson JA, Pessayre D, Lemasters JJ. Mechanisms of hepatotoxicity. *Toxicol Sci* 2002;65:166-176.
- Videla LA, Fernandez V, Tapia G, Varela P. Oxidative stress-mediated hepatotoxicity of iron and copper: role of Kupffer cells. *Biometals* 2003;16:103-111.
- Schwabe RF, Brenner DA. Mechanisms of liver injury. I. TNF-alpha-induced liver injury: role of IKK, JNK, and ROS pathways. *Am J Physiol Gastrointest Liver Physiol* 2006;290:G583-G589.
- Kim JS, He L, Qian T, Lemasters JJ. Role of the mitochondrial permeability transition in apoptotic and necrotic death after ischemia/reperfusion injury to hepatocytes. *Curr Mol Med* 2003;3:527-535.
- Christ WJ, Asano O, Robidoux ALC, Perez M, Wang Y, Dubuc GR, et al. E5531, a pure endotoxin antagonist of high potency. *Science* 1995;268:80-83.
- Swanson CA. Iron intake and regulation: implications for iron deficiency and iron overload. *Alcohol* 2003;30:99-102.
- Kohgo Y, Ohtake T, Ikuta K, Suzuki Y, Hosoki Y, Saito H, et al. Iron accumulation in alcoholic liver diseases. *Alcohol Clin Exp Res* 2005;29(Suppl):189S-193S.
- Petersen DR. Alcohol, iron-associated oxidative stress, and cancer. *Alcohol* 2005;35:243-249.
- Brewer GJ. Iron and copper toxicity in diseases of aging, particularly atherosclerosis and Alzheimer's disease. *Exp Biol Med (Maywood)* 2007;232:323-335.
- Imeryuz N, Tahan V, Sonmez A, Eren F, Uraz S, Yuksek M, et al. Iron preloading aggravates nutritional steatohepatitis in rats by increasing apoptotic cell death. *J Hepatol* 2007;47:851-859.
- Ma Y, de GH, Liu Z, Hider RC, Petrat F. Chelation and determination of labile iron in primary hepatocytes by pyridinone fluorescent probes. *Biochem J* 2006;395:49-55.
- Kerkweg U, Li T, de Groot H, Rauen U. Cold-induced apoptosis of rat liver cells in University of Wisconsin solution: the central role of chelatable iron. *HEPATOLOGY* 2002;35:560-567.
- Rauen U, Kerkweg U, de Groot H. Iron-dependent vs. iron-independent cold-induced injury to cultured rat hepatocytes: a comparative study in physiological media and organ preservation solutions. *Cryobiology* 2007;54:77-86.
- Rauen U, Petrat F, Sustmann R, de Groot H. Iron-induced mitochondrial permeability transition in cultured hepatocytes. *J Hepatol* 2004;40:607-615.
- Hochhauser E, Ben Ari Z, Pappo O, Chepurko Y, Vidne BA. TPEN attenuates hepatic apoptosis: ischemia/reperfusion injury and remote early cardiac dysfunction. *Apoptosis* 2005;10:53-62.
- Qian T, Nieminen AL, Herman B, Lemasters JJ. Mitochondrial permeability transition in pH-dependent reperfusion injury to rat hepatocytes. *Am J Physiol* 1997;273:C1783-C1792.
- Nieminen AL, Gores GJ, Bond JM, Imberti R, Herman B, Lemasters JJ. A novel cytotoxicity screening assay using a multiwell fluorescence scanner. *Toxicol Appl Pharmacol* 1992;115:147-155.
- Kim JS, Jin Y, Lemasters JJ. Reactive oxygen species, but not  $\text{Ca}^{2+}$  overload, trigger pH- and mitochondrial permeability transition-dependent death of adult rat myocytes after ischemia-reperfusion. *Am J Physiol Heart Circ Physiol* 2006;290:H2024-H2034.
- Carhuari R, Schwiers L, Ames BN. Detection of picomole levels of hydroperoxides using a fluorescent dichlorofluorescein assay. *Anal Biochem* 1983;136:111-116.
- Zahrbeldi G, Nieminen AL, al Ghoul K, Qian T, Herman B, Lemasters JJ. Progression of subcellular changes during chemical hypoxia to cultured rat hepatocytes: a laser scanning confocal microscopic study. *HEPATOLOGY* 1995;21:1361-1372.

27. Lemasters JJ, Trollinger DR, Qian T, Cascio WE, Ohata H. Confocal imaging of  $Ca^{2+}$ , pH, electrical potential, and membrane permeability in single living cells. *Methods Enzymol* 1999;302:341-358.
28. Breuer W, Epsztejn S, Millgram P, Cabantchik IZ. Transport of iron and other transition metals into cells as revealed by a fluorescent probe. *Am J Physiol* 1995;268:C1354-C1361.
29. Gagliardi S, Rees M, Farina C. Chemistry and structure-activity relationships of baflomycin A1, a potent and selective inhibitor of the vacuolar  $H^{+}$ -ATPase. *Curr Med Chem* 1999;6:1197-1212.
30. Nieminen AL, Saylor AK, Tefal SA, Herman B, Lemasters JJ. Contribution of the mitochondrial permeability transition to lethal injury after exposure of hepatocytes to *t*-butylhydroperoxide. *Biochem J* 1995;307:99-106.
31. Ying WL, Emerson J, Clarke MJ, Smadi DR. Inhibition of mitochondrial calcium ion transport by an oxo-bridged dinuclear ruthenium ammine complex. *Biochemistry* 1991;30:4949-4952.
32. Breuer W, Epsztejn S, Millgram P, Cabantchik IZ. Transport of iron and other transition metals into cells as revealed by a fluorescent probe. *Am J Physiol* 1995;268:C1354-C1361.
33. Liu ZD, Hider RC. Design of clinically useful iron(III)-selective chelators. *Med Res Rev* 2002;22:26-64.
34. Cederbaum AI. Oxygen radical generation by microsomes: role of iron and implications for alcohol metabolism and toxicity. *Free Radic Biol Med* 1989;7:559-567.
35. Britton RS, Leicester KL, Bacon BR. Iron toxicity and chelation therapy. *Int J Hematol* 2002;76:219-228.
36. Castilho RF, Meinicke AR, Almeida AM, Hermes-Lima M, Vercesi AE. Oxidative damage of mitochondria induced by Fe(II)citrate is potentiated by  $Ca^{2+}$  and includes lipid peroxidation and alterations in membrane proteins. *Arch Biochem Biophys* 1994;308:158-163.
37. Werneburg NW, Guicciardi ME, Bronk SF, Gores GJ. Tumor necrosis factor- $\alpha$ -associated lysosomal permeabilization is cathepsin B dependent. *Am J Physiol Gastrointest Liver Physiol* 2002;283:G947-G956.
38. Feldstein AE, Werneburg NW, Li Z, Bronk SF, Gores GJ. Bax inhibition protects against free fatty acid-induced lysosomal permeabilization. *Am J Physiol Gastrointest Liver Physiol* 2006;290:G1339-G1346.
39. Feldstein AE, Werneburg NW, Cambay A, Guicciardi ME, Bronk SF, Ryzdzewski R, et al. Free fatty acids promote hepatic lipotoxicity by stimulating TNF- $\alpha$  expression via a lysosomal pathway. *HEPATOLOGY* 2004;40:185-194.
40. Rossi L, Lombardo MF, Ciriolo MR, Rotilio G. Mitochondrial dysfunction in neurodegenerative diseases associated with copper imbalance. *Neurochem Res* 2004;29:493-504.
41. Nieminen AL, Byrne AM, Herman B, Lemasters JJ. Mitochondrial permeability transition in hepatocytes induced by *t*-BuOOH: NAD(P)H and reactive oxygen species. *Am J Physiol* 1997;272:C1286-C1294.
42. Persson HL, Yu Z, Tirosh O, Eaton JW, Brunk UT. Prevention of oxidant-induced cell death by lysosomotropic iron chelators. *Free Radic Biol Med* 2003;34:1295-1305.
43. She H, Xiong S, Lin M, Zandi E, Giulivi C, Tsukamoto H. Iron activates NF- $\kappa$ B in Kupffer cells. *Am J Physiol Gastrointest Liver Physiol* 2002; 283:G719-G726.
44. Tsukamoto H. Iron regulation of hepatic macrophage TNF $\alpha$  expression. *Free Radic Biol Med* 2002;32:309-315.
45. Xiong S, She H, Takeuchi H, Han B, Engelhardt JF, Barton CH, et al. Signaling role of intracellular iron in NF- $\kappa$ B activation. *J Biol Chem* 2003;278:17646-17654.
46. Wang GL, Semenza GL. Desferrioxamine induces erythropoietin gene expression and hypoxia-inducible factor 1 DNA-binding activity: implications for models of hypoxia signal transduction. *Blood* 1993;82:3610-3615.
47. Wenger RH. Cellular adaptation to hypoxia: O $_2$ -sensing protein hydroxylases, hypoxia-inducible transcription factors, and O $_2$ -regulated gene expression. *FASEB J* 2002;16:1151-1162.
48. Kurz T, Terman A, Brunk UT. Autophagy, ageing and apoptosis: the role of oxidative stress and lysosomal iron. *Arch Biochem Biophys* 2007;462: 220-230.
49. Ponka P, Beaumont C, Richardson DR. Function and regulation of transferrin and ferritin. *Semin Hematol* 1998;35:35-54.
50. Ponka P, Lok CN. The transferrin receptor: role in health and disease. *Int J Biochem Cell Biol* 1999;31:1111-1137.
51. Hentze MW, Muckenthaler MU, Andrews NC. Balancing acts: molecular control of mammalian iron metabolism. *Cell* 2004;117:285-297.
52. Mackenzie B, Garrick MD. Iron Imports. II. Iron uptake at the apical membrane in the intestine. *Am J Physiol Gastrointest Liver Physiol* 2005; 289:G981-G986.
53. Tabuchi M, Yoshimori T, Yamaguchi K, Yoshida T, Kishi F. Human NRAMP2/DMT1, which mediates iron transport across endosomal membranes, is localized to late endosomes and lysosomes in HEp-2 cells. *J Biol Chem* 2000;275:22220-22228.
54. Wildenthal K, Decker RS. The role of lysosomes in the heart. *Adv Myocardiol* 1980;2:349-358.
55. Ollinger K, Brunk UT. Cellular injury induced by oxidative stress is mediated through lysosomal damage. *Free Radic Biol Med* 1995;19:565-574.
56. Persson HL, Yu Z, Tirosh O, Eaton JW, Brunk UT. Prevention of oxidant-induced cell death by lysosomotropic iron chelators. *Free Radic Biol Med* 2003;34:1295-1305.
57. Yu Z, Persson HL, Eaton JW, Brunk UT. Intralysosomal iron: a major determinant of oxidant-induced cell death. *Free Radic Biol Med* 2003;34: 1243-1252.
58. Kurz T, Gustafsson B, Brunk UT. Intralysosomal iron chelation protects against oxidative stress-induced cellular damage. *FEBS J* 2006;273:3106-3117.
59. Werneburg NW, Guicciardi ME, Bronk SF, Gores GJ. Tumor necrosis factor- $\alpha$ -associated lysosomal permeabilization is cathepsin B dependent. *Am J Physiol Gastrointest Liver Physiol* 2002;283:G947-G956.
60. Flaumark T, Romslo I. Energy-dependent accumulation of iron by isolated rat liver mitochondria: requirement of reducing equivalents and evidence for a unidirectional flux of Fe(II) across the inner membrane. *J Biol Chem* 1975;250:6433-6438.

## トピックス

#### IV. C型慢性肝炎の抗ウイルス療法

### 2. C型慢性肝炎の進展と治療抵抗性

## 2) 宿主側因子の関与

池嶋 健一 柳沼 礼子 渡辺 純夫

## 要 旨

C型慢性肝炎の進展および治療抵抗性はウイルス量やHCVジェノタイプなどのウイルス側因子に加え、種々の宿主側因子により規定されている。人種、性別や年齢などに加え、メタボリックシンドローム (MetS) の諸因子やその肝臓での発現形である肝脂肪化が、C型肝炎においても肝線維化の進行やインターフェロン (IFN) 治療奏効性に寄与する因子として重要であることが最近注目されている。これらの宿主側因子の検証は病態進展や治療効果の予測に有用であるだけでなく、難治例に対する新たな抗ウイルス療法介入アプローチの確立にも繋がることが期待される。

〔日内会誌 97：69～74, 2008〕

**Key words** : chronic hepatitis C, interferon resistance, fatty liver, hypertension, metabolic syndrome

## はじめに

本邦におけるC型肝炎ウイルスキャリアは約200万人超と推定されており、C型肝炎患者の多くは感染後数十年の時間経過を経て肝硬変・肝細胞癌へと進行するため、積極的な抗ウイルス療法により病態進展を阻止する必要がある。C型肝炎に対する抗ウイルス療法は現時点ではインターフェロン (IFN) を用いた治療が唯一の選択肢であり、リバビリン (Riba) 製剤の併用やペグ化IFN製剤 (Peg-IFN) の登場により以前と比較するとその治療成績は格段に向上してきているものの、依然として難治例が多く存在する。特に我が国においてはIFN奏効性の悪い

ジェノタイプ1b型・高ウイルス量の症例が7割近くを占めており、現在の標準的なPeg-IFN+Riba併用療法でのウイルス持続陰性化 (SVR) 率が50%前後に留まっていることが大きな問題である。このようにIFN治療成績が必ずしも満足のいく状況ではないことの原因は多岐にわたるが、ウイルス側の因子に加えて種々の宿主側因子が影響を及ぼしていると考えられる。HCVのウイルス量やジェノタイプ、ウイルス遺伝子の変異などに関しては、採血により得られたウイルスの解析により詳細な検討が多く成されているが、宿主側因子の解析はより複雑で難度が高く、十分な検討がされているとは言い難い。しかし、肝の自然免疫系や線維化メカニズムに関する基礎研究の最近の進歩は目覚ましく、またメタボリックシンドローム (MetS) をはじめとする代謝系素因の肝病態への関与が大変注目されてい

いけじま けんいち、やぎぬま れいこ、わたなべ  
すみお：順天堂大学消化器内科

表 1. C型慢性肝炎の肝線維化進展を規定する遺伝的形質と非遺伝的要素

遺伝的形質	非遺伝的要素
HFE (遺伝性ヘモクロマトーシス遺伝子)	アルコール過剰摂取
Angiotensinogen	HIV および HBV の重複感染
TGF- $\beta$ 1	感染時期
TNF- $\alpha$	肝移植
ApoE	糖尿病・インスリン抵抗性
MEH (Microsomal epoxide hydroxylase)	肝脂肪化
MCP-1, MCP-2	性差
Factor V	抗ウイルス療法の奏効性

る。本稿ではC型肝炎の進展とIFN治療抵抗性に  
関わる宿主側因子について、MetSとの関連を中  
心に概説したい。

## 1. 年齢・性差とC型肝炎の肝線維化進行 およびIFN治療抵抗性

一般的にHCV感染から慢性肝炎を経て肝硬変  
に至るまでの期間は20~30年を要すると言われ  
ている。実際、20ないし30歳代で輸血などによ  
りHCVに感染し、50~60歳代以降に肝硬変を背  
景とした肝癌の発症を認めるといった経過は極  
めて典型的である。しかし、一方で50歳代以降  
になってHCVに初感染し、5~10年程度の経過で  
急速に肝硬変にまで進行する例も少なからず経  
験される。また、生下時ないし幼少期に感染し  
たと考えられるケースでも30歳代に肝硬変に至  
ることは稀である。これらのことはHCVの持続  
感染期間よりも病態進展が特定の年代、特に50  
歳代前後から急峻になることを示唆している。  
他方、C型慢性肝炎の進行には明らかな性差が認  
められ、男性と比較し女性では肝線維化の進展  
が緩徐であることが知られているが、女性でも  
50歳代以降に急速に肝炎の進行が見られるこ  
とが多い。女性では肝炎の進行が遅いことの一因  
として、女性ホルモン、特にエストロゲンが  
肝線維化に対して抑制的に作用することが動物  
実験の系では証明されている。しかし、閉経に  
伴うホルモン環境の変化がヒトにおけるC型肝炎

の進行を規定しているかどうかについては、必  
ずしも十分なエビデンスが確立しているとは言  
えない。

慢性肝疾患での肝線維化は、種々の遺伝形質  
および環境因子や合併疾患により規定されてい  
る<sup>1)</sup>。C型肝炎における肝線維化も、進展が極め  
て遅く肝硬変に至らない群と、短期間で急速に  
線維化が進行する群に大別することが出来る。  
このような違いが生じる原因としては、ウイル  
スに対する免疫反応の差異に加えて、生体の炎  
症や酸化ストレス、組織損傷修復機構に関わる  
様々な因子の違いが挙げられる(表1)。特に、  
最近ではMetS関連の諸因子や肝脂肪化が肝線維  
化進展にも寄与していることが注目されている。  
IFN治療効果に関しては、肝線維化進行例で奏効  
率が悪いことは数多くの臨床的検討から明らか  
である。線維化進展例では血小板や白血球数が  
低いことなどにより十分量のIFN投与が出来な  
いことがその一因となっていると考えられるもの  
の、難治性のメカニズムについては必ずしも十  
分には解明されていない。一方、C型慢性肝炎の  
IFN奏効性に関連する遺伝子変異についても数多  
くの報告があり、一塩基変異多型(SNP)解析が  
注目されている(表2)。

## 2. C型慢性肝炎における肝脂肪化とIFN 治療抵抗性

わが国でも欧米型生活習慣が一般的になり、